UNCLASSIFIED

AD

219760

UNCLASSIFIED

AEROELASTIC AND STRUCTURES

RESEARCH LABORATORY

MASSACHUSETTS INSTITUTE OF TECHNOLOGY

TECHNICAL REPORT 75-1

SIMILARITY LAWS REQUIRED FOR EXPERIMENTAL

AEROTHERMOELASTIC STUDIES

BY

JOHN M. CALLIGEROS

JOHN DUGUNDJI

FOR THE

OFFICE OF NAVAL RESEARCH

DEPARTMENT OF THE NAVY

CONTRACT NO. Nonr 1841 (46)

MAY, 1959

AEROELASTIC AND STRUCTURES RESEARCH LABORATORY

MASSACHUSETTS INSTITUTE OF TECHNOLOGY

TECHNICAL REPORT 75-1

SIMILARITY LAWS REQUIRED FOR EXPERIMENTAL
AEROTHERMOELASTIC STUDIES

BY

JOHN M. CALLIGEROS

JOHN DUGUNDJI

FC

FOR THE

OFFICE OF NAVAL RESEARCH

DEPARTMENT OF THE NAVY

CONTRACT NO. Nonr-1841(46)

MAY 1959

TABLE OF CONTENTS

LIST OF FIGURES

LIST OF PRINCIPAL SYMBOLS

a	speed of sound
C	plate extensional stiffness per unit length, $$\int_{-h/2}^{h/2} \frac{E}{1-\nu^2}\, dz$$
C_p	specific heat of body material
c_p	specific heat of gas at constant pressure
c_v	specific heat of gas at constant volume
D	plate bending stiffness per unit length, $$\int_{-h/2}^{h/2} \frac{E z^2}{1-\nu^2}\, dz$$
E	Young's Modulus
F	Airy Stress function
G	shear modulus
g	acceleration due to gravity
h	heat transfer coefficient; cross-section depth
J	torsional stiffness constant
K	heat conductivity of body material
k	heat conductivity of gas
L	characteristic length
M	free stream Mach number, U/a_∞
m	molecular weight; mass per unit area

M_T midplane thermal moment per unit length,

$$\int_{-\Lambda/2}^{\Lambda/2} \frac{E \alpha \Delta T z}{1 - \nu} \, dz$$

N_T midplane thermal force per unit length,

$$\int_{-\Lambda/2}^{\Lambda/2} \frac{E \alpha \Delta T}{1 - \nu} \, dz$$

n   length scale ratio, L_P/L_M ; normal direction to body surface

p   pressure

P_r free stream Prandtl number, $C_{P_\infty} \mu_\infty / k_\infty$

q   free stream dynamic pressure, $1/2 \, \rho_\infty U^2$

q_H heat flux per unit area

R   Universal gas constant

R_e free stream Reynolds number, $\rho_\infty U L / \mu_\infty$

S   web, rib spacing

T   temperature

t   time

U   free stream velocity

u, v, w   velocity components; displacement components

x, y, z   rectangular coordinates

α coefficient of thermal expansion

γ ratio of specific heats, C_P/C_ν

δ thickness

ϵ	emissivity
ϵ_x	component of strain
κ	thermal diffusivity,
λ	nondimensional time parameter, $\dfrac{2ht}{\rho_B C_{P_B} \delta_0}$
μ	viscosity of gas
ν	Poisson's ratio
ρ	density of gas
σ	Stefan-Boltzman constant
$\sigma_x, \sigma_y, \sigma_z$	normal stress components
$\tau_{xy}, \tau_{xz}, \tau_{yz}$	shearing stress components
ω	circular frequency

Subscripts

A	relating to aerodynamic forces
AW	adiabatic wall
B	relating to body
F	relating to non-aerodynamic forces
M	relating to model quantity
O	reference value
P	relating to prototype quantity
s	relating to skin
T	relating to tangential forces
w	relating to web
∞	free stream value

1. INTRODUCTION

The recent trend to high speed aircraft and missiles has subjected these vehicles to the additional phenomenon of aerodynamic heating. This heating must be considered in any analysis of the vehicle's structural integrity. Since experimental testing of small scale models can play an important role in supplementing and substantiating theoretical analysis, the need for a good understanding of the general similarity laws of this combined aerodynamic, thermal, and elasticity problem is apparent.

The present report reviews some of the basic similarity parameters of this combined aerothermoelastic problem and assesses their general significance. Also, it will attempt to indicate means of dealing with some of the conflicting requirements of the similarity parameters. For simplicity, the present study is limited to moderate temperatures (below about $1000^\circ F$ - i.e., $M < 3.5$) and considers only elastic behavior of the material.

A general summary of the overall high temperature aircraft structural problem can be found in Ref. 1, together with some comments regarding the use of models in high temperature structural design. The specific problem of aerothermoelastic similarity laws has also been studied by several investigators during the past six years. Refs. 2 through 10 give a list of some of the approaches to this problem.

1.1 The Aerothermoelastic Model

For flight at Mach numbers less than about 1.5 where one can neglect aerodynamic heating, the testing of cold aeroelastic models (in particular flutter models), has emerged as an indispensible aid in designing structures to avoid aeroelastic phenomena. There are two basically differ-

ent approaches to the use of models in aeroelastic development work. In one, the model tests are designed to evaluate coefficients to be inserted into the theories. In the other, the model tests are designed as analogues of the full scale problem. The latter approach is particularly desirable in proof testing specific aircraft configurations, and it is here that a thorough understanding of the similarity laws is necessary.

At the higher flight Mach numbers, it becomes necessary to include the effects of aerodynamic heating in any aeroelastic model test conducted to represent the full scale aircraft. One means of doing this is to first compute the loss in stiffness due to the aerodynamic heating, then to construct the model to conform to this reduced stiffness, and finally to test this reduced stiffness model in a conventional low stagnation temperature wind tunnel at the proper Mach number. This approach requires analytical computation of heating effects and also generally assumes separation into separate aerothermal and aeroelastic problems with no feedback interaction between the two. See the discussion in Ref. 1.

A more direct approach to this problem would be to construct a model and insert it directly into a high stagnation temperature wind tunnel. This aerothermoelastic model is thus subjected to the heating and airloads simultaneously. This approach requires a thorough knowledge of the similarity conditions for aerodynamic heating as well as aeroelasticity. As will be seen, the satisfaction of all the similarity conditions for an aerothermoelastic model is not generally possible except for a scale ratio of 1 : 1. Hence either some similarity condition will have to be relaxed in extrapolating the model to full scale or the model test will have to be used in the sense of evaluating coefficients to be inserted into various theories.

In addition to these complete aerothermoelastic models, "restricted purpose" models might be used to advantage to investigate certain well-defined phenomena. Aerodynamic heat transfer models, cold aeroelastic models, structural models, and cold aerodynamic stability derivative models are some well known examples of such "restricted purpose" models that can yield significant data on specific problem areas.

2. GENERAL AEROTHERMOELASTIC SIMILARITY LAWS

Various studies of the similarity laws associated with models placed in high stagnation wind tunnels are given in Refs. 2 to 10. Generally, these studies are made either by applying the Buckingham π theorem of dimensional analysis as in Refs. 6 and 9, or by examining the appropriate governing equations in non-dimensional form, as in Refs. 4, 5, and 7. The latter approach seems more flexible, particularly since the significance of the various non-dimensional parameters can be better ascertained. This approach will be utilized in this section.

Following Ref. 5, the general aerothermoelastic problem can be divided into three parts, namely, one dealing with the aerodynamic flow, one dealing with the heat conduction to the interior, and a third part dealing with the thermal stresses and external loads applied to the structure. The similarity relations associated with each of these parts will be treated in turn.

2.1 Aerodynamic Similarity

The two-dimensional flow[*] of a compressible viscous heat conducting perfect gas is characterized by the following equations,

$$\frac{\partial \rho}{\partial t} + \frac{\partial}{\partial x}(\rho u) + \frac{\partial}{\partial z}(\rho w) = 0 \tag{2.1}$$

$$\rho\left[\frac{\partial u}{\partial t} + u\frac{\partial u}{\partial x} + w\frac{\partial u}{\partial z}\right] = -\frac{\partial p}{\partial x} + \frac{2}{3}\frac{\partial}{\partial x}\left[2\mu\frac{\partial u}{\partial x} - \mu\frac{\partial w}{\partial z}\right] + \frac{\partial}{\partial z}\left[\mu\frac{\partial w}{\partial x} + \mu\frac{\partial u}{\partial z}\right] \tag{2.2}$$

---

[*] Two-dimensional flow is assumed here for simplicity in writing. The three-dimensional situation will not introduce any additional parameters.

$$\rho\left[\frac{\partial w}{\partial t} + u\frac{\partial w}{\partial x} + w\frac{\partial w}{\partial z}\right] = -\frac{\partial p}{\partial y} + \frac{2}{3}\frac{\partial}{\partial z}\left[2\mu\frac{\partial w}{\partial z} - \mu\frac{\partial u}{\partial x}\right] + \frac{\partial}{\partial x}\left[\mu\frac{\partial w}{\partial x} + \mu\frac{\partial u}{\partial z}\right] \tag{2.3}$$

$$\rho c_p\left[\frac{\partial T}{\partial t} + u\frac{\partial T}{\partial x} + w\frac{\partial T}{\partial z}\right] = \frac{\partial p}{\partial t} + u\frac{\partial p}{\partial x} + w\frac{\partial p}{\partial z} + \frac{\partial}{\partial x}\left(k\frac{\partial T}{\partial x}\right) + \frac{\partial}{\partial z}\left(k\frac{\partial T}{\partial z}\right)$$

$$+\mu\left\{2\left[\left(\frac{\partial u}{\partial x}\right)^2 + \left(\frac{\partial w}{\partial z}\right)^2\right] + \left[\frac{\partial w}{\partial x} + \frac{\partial u}{\partial z}\right]^2 - \frac{2}{3}\left[\frac{\partial u}{\partial x} + \frac{\partial w}{\partial z}\right]^2\right\} \tag{2.4}$$

$$p = \frac{R}{m}\rho T \tag{2.5}$$

where u, w represent the velocity components, T the temperature, ρ the density, p the pressure, μ the viscosity, k the heat conductivity, c_p the specific heat at constant pressure, R the universal gas constant, and m the molecular weight of the gas.

If now the following non-dimensional parameters are introduced,

$$\bar{x} = \frac{x}{L} \qquad\qquad \bar{z} = \frac{z}{L}$$

$$\bar{u} = \frac{u}{U} \qquad \bar{w} = \frac{w}{U} \qquad \bar{t} = \frac{t}{t_o}$$

$$\bar{p} = \frac{p}{p_\infty} \qquad \bar{\rho} = \frac{\rho}{\rho_\infty} \qquad \bar{T} = \frac{T}{T_o} \tag{2.6}$$

$$\bar{c}_p = \frac{c_p}{c_{p_\infty}} \qquad \bar{k} = \frac{k}{k_o} \qquad \bar{\mu} = \frac{\mu}{\mu_\infty}$$

where the subscript o denotes some reference value and the subscript ∞ denotes the free stream value, the above equations will reduce to,

$$\frac{\rho_\infty U}{L}\left[\left(\frac{L}{Ut_o}\right)\frac{\partial \bar{\rho}}{\partial \bar{t}} + \frac{\partial}{\partial \bar{x}}(\bar{\rho}\,\bar{u}) + \frac{\partial}{\partial \bar{z}}(\bar{\rho}\,\bar{w})\right] = 0 \tag{2.7}$$

$$\bar{\rho}\left[\left(\frac{L}{Ut_o}\right)\frac{\partial \bar{u}}{\partial \bar{t}} + \bar{u}\frac{\partial \bar{u}}{\partial \bar{x}} + \bar{w}\frac{\partial \bar{w}}{\partial \bar{z}}\right] = -\left(\frac{P_\infty}{\rho_\infty U^2}\right)\frac{\partial \bar{p}}{\partial \bar{x}} + \left(\frac{\mu_\infty}{\rho_\infty UL}\right)\left\{\frac{2}{3}\frac{\partial}{\partial \bar{x}}\left[2\bar{\mu}\frac{\partial \bar{u}}{\partial \bar{x}} - \bar{\mu}\frac{\partial \bar{w}}{\partial \bar{z}}\right]\right.$$

$$\left. + \frac{\partial}{\partial \bar{z}}\left[\bar{\mu}\frac{\partial \bar{w}}{\partial \bar{x}} + \bar{\mu}\frac{\partial \bar{u}}{\partial \bar{z}}\right]\right\} \tag{2.8}$$

$$\bar{\rho}\left[\left(\frac{L}{Ut_o}\right)\frac{\partial \bar{w}}{\partial \bar{t}} + \bar{u}\frac{\partial \bar{w}}{\partial \bar{x}} + \bar{w}\frac{\partial \bar{w}}{\partial \bar{z}}\right] = \text{etc.} \tag{2.9}$$

$$\bar{\rho}\,\bar{c}_p\left[\left(\frac{L}{Ut_o}\right)\frac{\partial \bar{T}}{\partial \bar{t}} + \bar{u}\frac{\partial \bar{T}}{\partial \bar{x}} + \bar{w}\frac{\partial \bar{T}}{\partial \bar{z}}\right] = \left(\frac{T_\infty}{T_o}\right)\left(\frac{P_\infty}{\rho_\infty T_o c_{p_\infty}}\right)\left[\left(\frac{L}{Ut_o}\right)\frac{\partial \bar{p}}{\partial \bar{t}} + \bar{u}\frac{\partial \bar{p}}{\partial \bar{x}} + \bar{w}\frac{\partial \bar{p}}{\partial \bar{z}}\right]$$

$$+ \left(\frac{k_\infty}{L\rho_\infty c_{p_\infty} U}\right)\left[\frac{\partial}{\partial \bar{x}}\left(\bar{k}\frac{\partial \bar{T}}{\partial \bar{x}}\right) + \frac{\partial}{\partial \bar{z}}\left(\bar{k}\frac{\partial \bar{T}}{\partial \bar{z}}\right)\right] \tag{2.10}$$

$$\bar{p} = \left(\frac{R\rho_\infty T_\infty}{m P_\infty}\right)\left(\frac{T_o}{T_\infty}\right)\bar{\rho}\,\bar{T} = \left(\frac{T_o}{T_\infty}\right)\bar{\rho}\,\bar{T} \tag{2.11}$$

Examination of the above equations reveals that if certain non-dimensional parameters are the same for a model and a prototype, then Eqs, (2.7) to (2.11) will be identical for both these cases and will have identical non-dimensional

solutions for the unknowns $\bar{u}$, $\bar{w}$, $\bar{T}$, $\bar{\rho}$ and $\bar{p}$. Hence measurements of $\bar{u}$, $\bar{w}$, $\bar{T}$, $\bar{\rho}$, and $\bar{p}$ on a model can then be used to find u, w, T, ρ, and p on the prototype by application of Eqs. (2.6). These non-dimensional parameters that must be identical are,

$$\frac{L}{Ut_o}$$

$$\frac{p_\infty}{\rho_\infty U^2} = \frac{1}{\gamma M^2}$$

$$\frac{\mu_\infty}{\rho_\infty UL} = \frac{1}{Re}$$

$$\left(\frac{T_\infty}{T_o}\right)\left(\frac{p_\infty}{\rho_\infty T_\infty c_{p_\infty}}\right) = \left(\frac{T_\infty}{T_o}\right)\left(\frac{c_{p_\infty} - c_{v_\infty}}{c_{p_\infty}}\right) = \left(\frac{T_\infty}{T_o}\right)\frac{\gamma - 1}{\gamma} \tag{2.12}$$

$$\frac{k_\infty}{\rho_\infty L c_{p_\infty} U} = \left(\frac{k_\infty}{c_{p_\infty}\mu_\infty}\right)\left(\frac{\mu_\infty}{\rho_\infty UL}\right) = \frac{1}{(P_r)(Re)}$$

$$\left(\frac{T_\infty}{T_o}\right)\frac{\mu_\infty U}{L\rho_\infty c_{p_\infty} T_\infty} = \left(\frac{T_\infty}{T_o}\right)\left(\frac{\mu_\infty}{\rho_\infty UL}\right)\left(\frac{U^2}{c_{p_\infty}T_\infty}\right) = \left(\frac{T_\infty}{T_o}\right)\frac{M^2}{Re}(\gamma - 1)$$

$$\frac{T_\infty}{T_o}$$

$$\overline{\overline{c_p}} \quad , \quad \overline{\overline{\mu}} \quad , \quad \overline{\overline{k}}$$

Thus similarity in the aerodynamic flow and heating will prevail if the following nine parameters are maintained equal,

Free stream Mach number, $\quad M = U/a_\infty$

Free stream Reynolds number, $Re = \dfrac{\rho_\infty UL}{\mu_\infty}$

Free stream Prandtl number, $\quad P_r = \dfrac{c_{p\infty}\mu_\infty}{k_\infty}$

Ratio of Specific heats, $\quad \gamma$

Unsteady Flow parameter, $\quad Ut_o/L$ $\qquad$ (2.13)

Reference Temperature ratio, $\quad T_o/T_\infty$

$$\bar{\bar{c}}_p \;,\; \bar{\mu}\,,\; \bar{k}$$

Usually the aerodynamic heating model test will be made in the same medium (air) as the prototype. In this case, the γ's are the same. Also, the P_r generally doesn't vary much over a large temperature range. The unsteady term Ut_o/L and reference temperature ratio T_o/T_∞ serve to define the reference time t_o and the reference temperature[*] T_o respectively. The quantities $\bar{\bar{c}}_p$, $\bar{\mu}$, $\bar{k}$ depend only on the temperature T. If the free stream temperature is chosen the same for both model and prototype in the same gas, these non-dimensional quantities will always be the same. If the T_∞'s are somewhat different, these conditions can still be maintained over a low range of temperatures since c_p does not vary much between 0 - 1000°F and k and μ can be expressed as $k \sim T^{\alpha_1}$ and $\mu \sim T^{\alpha_2}$ over this limited range.

Under all these above conditions the aerodynamic heating similarity reduces to the requirements mainly of equal Mach number M and equal Reynolds number Re for the flow.

In addition to the differential equations, the boundary conditions should also be investigated. The boundary conditions at the surface of the body are,

---

[*] It will be convenient when later dealing with heat conduction similarity to choose some reference temperature other than the free stream temperature.

$$u = 0 \quad , \quad w = 0$$

$$(T)_{AIR} = (T)_{BODY}$$

$$q_H = \left(k \frac{\partial T}{\partial n}\right)_{AIR} = (q_H)_{BODY} \qquad\qquad (2.14)$$

where q_H is the heat flux per unit area and n is the normal direction to the body surface. Introducing the non-dimensional quantities of Eq. (2.6) into the above will result in the requirement that prototype and model have the same external geometric boundary shape,[*] and that the air temperature be equal to the body temperature at the wall. The significance of the condition on heat flux q_H will be considered in the next section.

The preceding development was based on laminar flow. The similarity requirements are assumed to be the same for turbulent flow. In this connection, the surface roughness of the model and the turbulence level of the tunnel should be kept small to conform with the prototype, and to help locate transition at a somewhat similar location.

2.2 Heat Conduction Similarity

The primary means of heat flow in the interior of the body is by conduction. The conduction of heat is characterized by the classical Fourier equation

$$\frac{\partial}{\partial x}\left(K \frac{\partial T}{\partial x}\right) + \frac{\partial}{\partial y}\left(K \frac{\partial T}{\partial y}\right) + \frac{\partial}{\partial z}\left(K \frac{\partial T}{\partial z}\right) = \rho_o \, C_p \frac{\partial T}{\partial t} \qquad\qquad (2.15)$$

---

[*] This condition is automatically fulfilled by a scaled model. However, it also requires that any subsequent structural deflections also be in scale.

where K, Cp, and ρ_B are the heat conductivity, specific heat, and density, respectively, of the body material. Introducing the non-dimensional parameters

$$\bar{x} = \frac{x}{L} \quad , \quad \bar{y} = \frac{y}{L} \quad , \quad \bar{z} = \frac{z}{L}$$

$$\bar{T} = \frac{T}{T_o} \quad , \quad \bar{t} = \frac{t}{t_o}$$

$$\bar{\bar{K}} = \frac{K}{K_o} \quad , \quad \bar{C}_P = \frac{C_P}{C_{P_o}}$$

(2.16)

the heat conduction equation becomes

$$\frac{\partial}{\partial \bar{x}}\left(\bar{\bar{K}}\frac{\partial \bar{T}}{\partial \bar{x}}\right) + \frac{\partial}{\partial \bar{y}}\left(\bar{\bar{K}}\frac{\partial \bar{T}}{\partial \bar{y}}\right) + \frac{\partial}{\partial \bar{z}}\left(\bar{\bar{K}}\frac{\partial \bar{T}}{\partial \bar{z}}\right) = \left(\frac{\rho_B C_{P_o} L^2}{K_o t_o}\right) \bar{\bar{C}}_P \frac{\partial \bar{T}}{\partial \bar{t}}$$

(2.17)

Here, the resulting non-dimensional parameters that must be equal for both model and prototype are

$$\frac{K_o t_o}{L^2} \quad , \quad \bar{K} \quad , \quad \bar{\bar{C}}_P$$

(2.18)

where $\kappa_o = K_o/\rho_B C_{P_o}$ is the thermal diffussivity of the material. The first parameter is the Fourier number and serves to define the characteristic time of the heat conduction process. The latter two parameters, $\bar{\bar{K}}$ and $\bar{\bar{C}}_p$, are automatically simulated if the same materials and same temperatures are utilized for both model and prototype. If this is not the case, some relaxation in true similarity will generally result, although this may not be very important in certain cases (quite often, the assumption of a constant K and C_p yields good results for not too large temperature ranges).

The boundary condition for the heat conduction problem is

$$\left(K \frac{\partial T}{\partial \eta} \right)_{BODY} = \left(k \frac{\partial T}{\partial \eta} \right)_{AIR} - \epsilon \sigma T^4 \qquad (2.19)$$

at the body surface (see also Eq. (2.14)). In the above, the right hand side represents, respectively, the heat input from the aerodynamic heating, and the heat loss due to radiation from the body. Non-dimensionalizing this as before yields

$$\left(\bar{K} \frac{\partial \bar{T}}{\partial \bar{\eta}} \right)_{BODY} = \left(\frac{k_\infty}{K_0} \right) \left(\bar{k} \frac{\partial \bar{T}}{\partial \bar{\eta}} \right)_{AIR} - \left(\frac{\epsilon_0 T_0^3 L}{K_0} \right) \bar{\epsilon} \sigma \bar{T}^4 \qquad (2.20)$$

The non-dimensional parameters that must be equal for both model and prototype for simulation of the boundary condition are

$$\frac{k_\infty}{K_0} \quad , \quad \frac{\epsilon_0 T_0^3 L}{K_0} \quad , \quad \bar{k} \, , \, \bar{K} \, , \, \bar{\epsilon} \qquad (2.21)$$

The non-dimensional temperature gradient $(\partial \bar{T}/\partial \bar{n})_{air}$ of Eq. (2.20) must be the same for both model and prototype. This will be assured if the previous similarity conditions on the aerodynamics are fulfilled.

The first condition of Eq. (2.21) expresses the ratio of heat flux from the boundary layer to the heat conducted into the body and the second condition expresses the ratio of heat lost by radiation to heat conducted into the body. The k_∞/K_0, $\bar{k}$, and $\bar{K}$ conditions will be automatically satisfied if the same materials, gases, and temperatures are utilized for the model and prototype. If not, some relaxation of the similarity conditions as discussed before will result.

Other boundary conditions such as at an insulated wall (K $\frac{\partial T}{\partial n}$ = 0) will not introduce any additional similarity parameters.

For heat conduction similarity then, the model and prototype must be geometrically similar, the temperature distribution $\overline{T}_{air}$ must be similar, and the parameters of Eqs. (2.18) and (2.21) must be the same for both. If radiation is assumed negligible, and if model and prototype are of the same materials and temperatures and in the same gas mediums, the heat conduction similarity requirements reduce simply to maintaining the same Fourier number $\kappa_o t_0/L^2$. Thus at corresponding non-dimensional times the non-dimensional temperature $\overline{T}$ will be the same for model and prototype at corresponding points in the body.

2.3 Stress and Deflection Similarity

The equations governing the stresses and deflections of a three-dimensional heated elastic body can be written in terms of three equilibrium and six stress-displacement equations. The first of the three equilibrium equations is

$$\frac{\partial \sigma_z}{\partial z} + \frac{\partial \tau_{xz}}{\partial x} + \frac{\partial \tau_{yz}}{\partial y} = \rho_o \frac{\partial^2 w}{\partial t^2} - \rho_o g \tag{2.22}$$

where the terms on the right hand side represent the inertial loading and gravity loading, respectively. The first of the six stress-displacement equations, allowing for large structural deflections, is

$$\varepsilon_x = \frac{\partial u}{\partial x} + \frac{1}{2}\left[\left(\frac{\partial u}{\partial x}\right)^2 + \left(\frac{\partial v}{\partial x}\right)^2 + \left(\frac{\partial w}{\partial x}\right)^2\right] = \frac{1}{E}\left[\sigma_x - \nu(\sigma_y + \sigma_z)\right] + \alpha \Delta T \tag{2.23}$$

All the remaining equations are similar in form to equations (2.22) and (2.23). In the above, ρ_B is the density of the material, E is the modulus of elasticity, ν is Poisson's ratio, α is the coefficient of thermal expansion, and ΔT is the temperature rise above some fixed initial value. The unknowns are the six stresses σx, σy, σz, τxy, τxz, τyz, and the three displacements u, v, w. The above equations are nonlinear in the displacements u, v, w, but it has been assumed that the stress-strain relationship is linear.

If now the following non-dimensional parameters are introduced

$$\bar{\sigma}_x = \frac{\sigma_x}{\sigma_o} \quad , \quad \bar{\sigma}_y = \frac{\sigma_y}{\sigma_o} \quad , \quad \bar{\sigma}_z = \frac{\sigma_z}{\sigma_o} \quad , \quad \bar{T} = \frac{T}{T_o}$$

$$\bar{\tau}_{xy} = \frac{\tau_{xy}}{\sigma_o} \quad , \quad \bar{\tau}_{zx} = \frac{\tau_{zx}}{\sigma_o} \quad , \quad \bar{\tau}_{yz} = \frac{\tau_{yz}}{\sigma_o} \quad , \quad \bar{t} = \frac{t}{t_o}$$

$$\bar{x} = \frac{x}{L} \quad , \quad \bar{y} = \frac{y}{L} \quad , \quad \bar{z} = \frac{z}{L} \quad , \quad \bar{u} = \frac{u}{u_o} \qquad (2.24)$$

$$\bar{v} = \frac{v}{u_o} \quad , \quad \bar{w} = \frac{w}{u_o} \quad , \quad \bar{\bar{E}} = \frac{E}{E_o}, \quad \bar{\bar{\alpha}} = \frac{\alpha}{\alpha_o}, \quad \bar{\bar{\nu}} = \frac{\nu}{\nu_o}$$

the above equations become

$$\frac{\partial \bar{\sigma}_z}{\partial \bar{z}} + \frac{\partial \bar{\tau}_{xz}}{\partial \bar{x}} + \frac{\partial \bar{\tau}_{yz}}{\partial \bar{y}} = \left(\frac{\rho_B \, u_o L}{\sigma_o \, t_o^2} \right) \frac{\partial^2 \bar{w}}{\partial \bar{t}^2} - \frac{\rho_B \, g L}{\sigma_o} \qquad (2.25)$$

$$\frac{\partial \bar{u}}{\partial \bar{x}} + \frac{1}{2} \left(\frac{u_o}{L} \right) \left[\left(\frac{\partial \bar{u}}{\partial \bar{x}} \right)^2 + \left(\frac{\partial \bar{v}}{\partial \bar{x}} \right)^2 + \left(\frac{\partial \bar{w}}{\partial \bar{x}} \right)^2 \right] =$$

$$\left(\frac{\sigma_o L}{E_o \, u_o} \right) \frac{1}{\bar{\bar{E}}} \left[\bar{\sigma}_x - \bar{\bar{\nu}} \nu_o \left(\bar{\sigma}_y + \bar{\sigma}_z \right) \right] + \left(\frac{\alpha_o \, T_o L}{u_o} \right) \bar{\bar{\alpha}} \Delta \bar{T} \qquad (2.26)$$

Equations (2.25) and (2.26) introduce the following non-dimensional parameters

$$\frac{\rho_B \, u_o L}{\sigma_o \, t_o^2} \quad , \quad \frac{\sigma_o L}{E_o \, u_o} \quad , \quad \frac{\alpha_o \, T_o \, L}{u_o} \quad , \quad \frac{u_o}{L} \quad , \quad \frac{\rho_B \, g \, L}{\sigma_o}$$

$$\bar{\bar{E}}, \quad \bar{\bar{\alpha}}, \quad \bar{\bar{\nu}}, \quad \nu_o$$

(2.27)

The non-dimensional temperature distribution $\bar{T}$ of Eq. (2.26) must be the same for model and prototype. This will be assured if the previous similarity conditions on the aerodynamics and heat conduction are fulfilled.

The first condition of Eq. (2.27) represents a condition on dynamics (for static problems this is neglected), while the second and third conditions represent the major requirements on static stress-deflection similarity. The parameter u_o/L requires the displacements of the structure to be in the same scale as the characteristic dimensions of the body and is important when considering large deflections. If u_o/L is maintained separately then the first three parameters of Eq. (2.27) are reduced to

$$\frac{\rho_B \, L^2}{\sigma_o \, t_o^2} \quad , \quad \frac{\sigma_o}{E_o} \quad , \quad \alpha_o \, T_o$$

(2.28)

However, if the assumption of small deflections can be made, the second term of the left hand side of Eq. (2.26) may be neglected and the parameter u_o/L no longer appears by itself. Thus, under small deflections, the structural deformations need not be scaled for stress-deflection similarity, and the parameters of Eq. (2.28) will appear in combination with u_o/L

as in Eq. (2.27).[*] The fifth parameter of Eq. (2.27) arises
from the gravitational forces. The last four conditions of
Eq. (2.27) are automatically satisfied if the same materials
at the same temperature are used. Otherwise, as before,
some relaxation of similarity will result.

For this elastic body, the boundary conditions at
the surface can be stated either in terms of prescribed dis-
placements or prescribed normal and tangential stresses.
Either

$$u = (u) \text{ prescribed}, \quad v = (v) \text{prescribed}, \quad w = (w) \text{ prescribed}$$

or

$$\sigma_n = (\sigma_n)_{\text{prescribed}} = p_A + p_F$$

$$\sigma_T = (\sigma_T)_{\text{prescribed}}$$

$$(2.29)$$

The displacement boundary conditions do not intro-
duce any new parameters. The normal stress boundary condi-
tion above (in which p_A represents the imposed aerodynamic
pressure distribution, and p_F any additional applied non-
aerodynamic loading), is generally the principal boundary
condition and it can be non-dimensionalized to give,

$$\overline{\sigma_n} = \frac{p_\infty \overline{p_A} + p_F}{\sigma_o}$$

$$(2.30)$$

where $\overline{p}_A = p_A/p_\infty$. Similarity requires that the parameter
$\overline{\sigma}_n$ as given above must be equal on both model and prototype.
The $\overline{p}_A$ term appearing in $\overline{\sigma}_n$ will itself be similar if the
previous similarity conditions on the aerodynamics are ful-
filled.

----

[*] Note however, that consideration of aerodynamic similarity,
(see section 2.1), requires generally that u_∞/L be scaled.

It is to be noted that the similarity condition on $\bar{\sigma}_n$ involves the sum of $\bar{p}_A$ (p_∞ / σ_0) and (p_F/σ_0). Since generally the aerodynamic pressure distribution $\bar{p}_A$ is not known in advance, particularly in aeroelastic type models, the maintenance of $\bar{\sigma}_n$ similarity requires that the parameters

$$\frac{p_\infty}{\sigma_0} \quad , \quad \frac{p_F}{\sigma_0} \tag{2.31}$$

must each be maintained similar individually (the $\bar{p}_A$ already being maintained from aerodynamic similarity). However, in certain non-aeroelastic type tests where $\bar{p}_A$ can possibly be estimated, similarity can be achieved through Eq. (2.30) without the more restrictive requirements of Eq. (2.31).

Assuming that the temperature distribution $\bar{T}$ in the body and the aerodynamic pressure distribution $\bar{p}_A$ have been simulated, the parameters for stress and deflection similarity are given by Eqs. (2.27) and (2.30).

2.4 Summary of General Similarity Requirements

The general similarity parameters for aerothermoelastic modeling derived in the preceeding sections may be summarized as follows

a) External Aerodynamic Flow

$$M, Re, \frac{U t_0}{L}, P_r, \gamma, \bar{\bar{c}}_p, \bar{\bar{\mu}}, \bar{\bar{k}}, \frac{T_0}{T_\infty}, \frac{u_0}{L} \tag{2.32}$$

b) Heat Conduction

$$\frac{k_\infty}{K_0}, \frac{K_0 t_0}{L^2}, \frac{\epsilon_0 T_0^3 L}{K_0}, \bar{\bar{K}}, \bar{\bar{C}}_p, \bar{\epsilon}, \bar{\bar{k}} \tag{2.33}$$

c) Stress and Deflection

$$\frac{\sigma_o L}{E_o u_o} \;,\; \frac{\alpha_o T_o L}{u_o} \;,\; \frac{u_o}{L} \;,\; \frac{p_\infty \bar{P}_A + p_F}{\sigma_o}$$

$$\frac{\rho_B u_o L}{\sigma_o t_o^2} \quad,\quad \frac{\rho_B g L}{\sigma_o} \quad,\quad \bar{\bar{E}},\; \bar{\alpha},\; \bar{\nu},\; \nu_o \qquad\qquad (2.34)$$

These parameters are for the most general time dependent aerothermoelastic problem. They have been derived subject to the assumptions stated previously, and apply generally to elastic bodies below about 1000°F (i.e., M less than about 3.5).

It is possible, by suitable combinations, to alter some of the above similarity parameters into more compact and familiar forms. The u_o/L condition of Eqs. (2.32) and (2.34) can be introduced into the 1st, 2nd and 5th parameters of Eq. (2.34), to result in σ_o/E_o, $\alpha_o T_o$, and $\rho_B L^2/\sigma_o t_o^2$ respectively. The $(p_\infty \bar{P}_A + p_F)/\sigma_o$ parameter of Eq. (2.34), as discussed in section 2.3, implies the maintenance of the separate parameters p_∞/σ_o and p_F/σ_o. The p_∞/σ_o parameter, which then may serve to define the reference stress level σ_o, can be combined with the σ_o/E_o to yield the basic aeroelastic similarity parameter p_∞/E_o. This basic aeroelastic parameter expresses the ratio of aerodynamic forces to stiffness forces[*]. The parameter $\rho_B L^2/\sigma_o t_o^2$ can also be transformed, by combination with the similarity conditions $U t_o/L$,

---

[*] It could also have been expressed, by further combination with the perfect gas relation $p_\infty = \rho_\infty U^2/\gamma M^2$ and the and M similarity relations, in the alternate form q/E_o, where q is the dynamic pressure.

p_∞/σ_0, M, γ, and the perfect gas relation $p_\infty = \rho_\infty U^2/\gamma M^2$, into the simple form ρ_B/ρ_∞, which is the mass density ratio parameter important in flutter work. Similarly, the parameter $\rho_0 gL/\sigma_0$ can be changed, by combination with $\rho_B L^2/\sigma_0 t_0^2$ and Ut_0/L, into the form U^2/gL. This may be identified with the Froude number, which expresses the ratio of gravity forces to aerodynamic forces.

The general aerothermoelastic similarity parameters of Eqs. (2.32), (2.33), and (2.34) may be rewritten in terms of these above combined alternate forms as,

$$M, \ R_e, \ \frac{p_\infty}{E_0}, \ \frac{\rho_0}{\rho_\infty}, \ \frac{k_\infty}{K_0}, \ \alpha_0 T_0, \ P_r$$

$$\gamma, \ \frac{E_0 T_0 L^3}{K_0}, \ \frac{U^2}{gL}, \ \nu_0, \ \bar{\bar{k}}, \ \bar{\bar{c}}_p, \ \bar{\bar{\mu}}, \ \bar{\bar{K}}, \ \bar{\bar{C}}_p \qquad (2.35)$$

$$\bar{\bar{E}}, \ \bar{\bar{\alpha}}, \ \bar{\bar{\nu}}, \ \bar{\bar{\epsilon}}, \ \frac{Ut_0}{L}, \ \frac{K_0 t_0}{L^2}, \ \frac{u_0}{L}, \ \frac{p_\infty}{\sigma_0}, \ \frac{p_F}{\sigma_0}, \ \frac{T_0}{T_\infty}$$

The first six parameters of the above are the principal conditions to be satisfied for aerothermoelastic similarity. The next five are generally somewhat weaker requirements. The next nine double-barred quantities reflect the variations in the parameters for conditions departing from the reference temperature T_0. For same model and prototype materials at the same temperatures, these are all identically satisfied. The remaining six parameters serve to define the reference values of t_0, u_0, σ_0 and T_0 to be used in the non-dimensionalizations. For the case of static aerothermoelastic models, the parameters ρ_0/ρ_∞, Ut_0/L can be dropped in the above, and the Froude number parameter U^2/gL will be replaced

by the original $\beta_B g^L/\sigma_o$ parameter of Eq. (2.34).

To investigate the application of the similarity parameters of Eq. (2.35), consider an experiment in which a scaled model is constructed of the same material and tested in the same gas and at the same free stream temperature as the prototype. It is assumed that the model will represent a static aerothermoelastic test and that the effects of radiation, gravity forces, and all non-aerodynamic loads P_F on both model and prototype are negligible. The model scale factor is designated by

$$\eta = \frac{L_P}{L_M} \tag{2.36}$$

where the subscript P denotes a prototype quantity and M a model quantity.

Under the above stated conditions, the similarity parameters of Eq. (2.35) reduce to,

$$M, \quad R_e, \quad \frac{P_o}{E_o}, \quad \frac{K_o t_o}{L^2}, \quad \frac{U_o}{L}, \quad \frac{P_\infty}{\sigma_o} \tag{2.37}$$

The following relations will be obtained between model and prototype quantities by maintaining all the above similarity conditions, except for the P_o/E_o condition,

$$\left(T_\infty\right)_M = \left(T_\infty\right)_P$$

$$(M)_M = (M)_P$$

$$(U)_M = (U)_P$$

$$(P_\infty)_M = \eta\,(P_\infty)_P$$

$$(\rho_\infty)_M = \eta\,(\rho_\infty)_P$$

$$(t_o)_M = \frac{1}{n^2}(t_o)_P$$

$$(u_o)_M = \frac{1}{n}(u_o)_P \qquad (2.38)$$

$$(\sigma_o)_M = n(\sigma_o)_P$$

The remaining p_o/E_o condition, which arises from the aero-dynamic forces on the body, will result in the relation,

$$(p_\infty)_M = (p_\infty)_P \qquad (2.39)$$

This condition contradicts the fifth condition of Eqs. (2.38) which arose from consideration of the Reynolds number condition. Hence for this simplified case of similar materials, similar gas, and similar temperatures in a static aerothermo-elastic test, conflicts arise among the similarity parameters, and one is unable to correctly simulate the prototype situation. This is also pointed out in Refs. 3, 5, 6, 7, 8 and 10.

Three other conflicting requirements, though generally less severe, would also have arisen had the more general dynamic aerothermoelastic case been considered. The first would have been a conflict in the characteristic times t_o resulting from the Ut_o/L and $\kappa_o t_o/L^2$ conditions for same materials. The former would have given a $(t_o)_M/(t_o)_P$ ratio of $1/n$ rather than the $1/n^2$ of the latter. This is not, however, a serious conflict because of the substantially different time constants associated with the vibrational and aero-dynamic phenomena (very short) and those of the thermal heating phenomena (quite long). Only if these are of about the same order of magnitude and if mutual coupling is possible

between these two phenomena would it be necessary to have a single common reference time t_o for the specific aerothermoelastic test. A second conflicting requirement might arise from the radiation $\epsilon_o T_o^3 L / K_o$ condition. For these similar materials at the same temperatures, the scale ratio would prevent satisfaction of this. Unless rather high temperatures are involved though this radiation would tend to be unimportant. Even then it might be alleviated to some extent by altering the surface characteristics and hence the emissivity ϵ of the model somewhat. Another source of conflict lies in the Froude number $U^2 / g L$. In most aeroelastic problems though this effect is small. The possible conflict involving the mass density ratio ρ_o / ρ_∞ can be alleviated somewhat by adding weights artificially to built-up type models.

However, the fundamental conflict in similarity remains that concerning the Mach number M, Reynolds number Re, and aeroelastic parameter ρ_∞ / E_o , and means of getting about this must be investigated.

One means of doing this is to attempt to use different model and prototype materials, in different gases, and at different temperatures. This approach is studied in Section 3.

Another approach is to develop less restrictive similarity parameters by considering more specialized situations than the very general ones given here for the aerodynamics, heat conduction, and stress-deflections. For these specialized situations it is possible to develop similarity laws permitting even geometrical distortions of the scaling down process. This approach which has been successful in developing, for example, cold flutter model techniques, is explored in Section 4.

A further approach to this conflict is to relax one of the requirements for similarity. Either the M, the

Re, or the f_0/E_0 requirement can be left unsatisfied. Consideration of the specialized similarity situations mentioned above may help give a better clue as to what parameters are important in considering specific types of phenomena, and what parameters may therefore be dropped. For example, the Re requirement can be shown to be associated mainly with the aerodynamic heating, and if this heating is unimportant, the Re requirement can be dropped. This is effectively what is done in ordinary cold aeroelastic testing. Or, if the aerodynamic loadings and subsequent structural distortions were not too important, the f_0/E_0 requirement could be disregarded. This is done in ordinary heat transfer and friction studies on models. Such types of "restricted purpose" model tests can be of use in investigating carefully delineated problems. The consequences of relaxing some parameters are discussed in Section 5.

It is of interest to note that another means of resolving this conflict between M, Re, and f_0/E_0 is possible in certain non-aeroelastic cases by placing additional non-aerodynamic surface loads f_F on the model. As discussed in Section 2.3, the normal stress similarity parameter is more generally $\overline{\sigma}_n$. Using this relation, the separate f_0/E_0 parameter of Eq. (2.35) will be replaced by the combined requirement,

$$\frac{f_0 \, \overline{p}_A + f_F}{E_0} \tag{2.40}$$

Appling this to a prototype without additional loads f_F and a model with additional loads, gives

$$\left(\frac{f_0 \, \overline{p}_A + f_F}{E_0} \right)_M = \left(\frac{f_0 \, \overline{p}_A}{E_0} \right)_P \tag{2.41}$$

This will result in the requirement of placing additional external loadings $(p_F)_m$ over the model of magnitude

$$(p_F)_m = (1-n)(p_A)_p \tag{2.42}$$

where $(p_A)_p$ is the presumed known aerodynamic pressure distribution. In an aeroelastic type model, the determination of, and the supplying of this additional surface loading might present considerable difficulty.

3. CONSIDERATION OF DIFFERENT MATERIALS AND DIFFERENT GASES

3.1 Different Materials

In the preceding section the similarity parameters of the general aerothermoelastic problem were derived and some of the inherent conflicts leading to the requirement of length scale ratios of 1 were indicated. It is of interest to investigate the use of different model and prototype materials and gases other than air for the test medium in matching these parameters. With this approach model stream temperatures need not also equal prototype stream temperatures and length scale ratios greater than 1 are generally possible.

The parameters required for similarity are given in Eq. (2.35). The principal similarity parameters to be matched here will be the M, Re, ρ_∞/E_0, k_∞/K_0, and $\alpha_0 T_0$ conditions. In attempting to match these, it is convenient to transform the Re requirement by introduction of the perfect gas law, Eq. (2.5), and combining with the M and ρ_∞/E_0 requirements into the new parameter,

$$\frac{L E_0}{\mu_\infty} \sqrt{\frac{\gamma m}{T_0}} \tag{3.1}$$

From the above, it can be seen that mutual satisfaction of the M, Re, and ρ_∞/E_0 conditions will result only for scale ratios of

$$\frac{L_P}{L_M} = \frac{\left(\frac{E_0}{\mu_\infty}\sqrt{\frac{\gamma m}{T_0}}\right)_M}{\left(\frac{E_0}{\mu_\infty}\sqrt{\frac{\gamma m}{T_0}}\right)_P} \tag{3.2}$$

Thus to achieve scale ratios greater than 1 it is desireable for the model material to have a higher modulus of elasticity

than the prototype and to use a gas heavier than air in the
tunnel at a lower temperature than the prototype.

In addition to satisfying M, Re, ρ_o/E_o, k_o/K_o
and $\alpha_o T_o$, the density ratio ρ_o/ρ_∞ should also be satisfied
(for dynamic tests only) as well as the non-dimensional mate-
rial and fluid properties $\bar{\bar{K}}$, $\bar{\bar{C}}_p$, $\bar{\bar{E}}$, $\bar{\bar{\alpha}}$, $\bar{\bar{\nu}}$, $\bar{\bar{k}}$, $\bar{\bar{c}}_p$, $\bar{\bar{\mu}}$.
The ρ_o/ρ_∞ parameter can often be manipulated by addition
of weights to built-up type structures. In satisfying the
latter double-barred parameters one is essentially matching
the slopes of model and prototype materials at the reference
temperatures $(T_o)_m$ and $(T_o)_p$. This is extremely difficult
and the problem may be facilitated by selecting T_o to lie
somewhere in the neighborhood of the expected maximum temper-
ature. In this manner $\bar{\bar{K}}$, $\bar{\bar{E}}$, $\bar{\bar{\alpha}}$ etc. are approximately
one, in this neighborhood,[*] the error depending on the differ-
ences in slopes of material properties. Of course, when the
same materials, gas, and temperatures are utilized these
quantities are automatically satisfied. It should be noted
that if a material or fluid property, λ, can be represented
by a temperature dependence of the form

$$\lambda \sim T^\omega \tag{3.3}$$

for some temperature range, then $\bar{\bar{\lambda}}$ will be automatically
satisfied since T/T_o is the same for model and prototype for
temperature similarity. The radiation condition and Froude
number will be assumed to be negligible here.

---

[*] The fluid properties $\bar{k}$, $\bar{\mu}$, $\bar{c}_f$, which are referred to
free stream temperature rather than the reference tempera-
ture T_o, are not 1. However, these properties are repre-
sentible in the form of Eq. (3.3) for this temperature
range (0 to 1000°F) and hence these quantities are also
generally satisfied.

Five structural materials, aluminum, magnesium, stainless steel, inconel-x, and titanium have been considered with respect to being used either as prototype or model materials. Material properties for these are given, for example, in Refs. 26, 27 and 28. For these materials and for air as the wind tunnel gas, the parameters k_∞/K_0, $\alpha_0 T_0$, and Eq. (3.2) have been plotted as a function of T_0 in Figs. 1, 2, and 3.[*] These plots illustrate concisely the difficulties encountered in satisfying the parameters for general similarity. Figure 2 shows that similar materials will satisfy the $\alpha_0 T_0$ condition only if model and prototype temperatures are the same. However, Fig. 3 shows that if similar materials and similar temperatures are utilized the scale ratio must be 1. Thus to simulate the $\alpha_0 T_0$ condition along with M, Re and P_∞/E_0 for scale ratios greater than 1, model and prototype materials and temperatures must be different. Figure 1 shows that the k_∞/K_0 condition cannot be satisfied if aluminum or magnesium are used for matching with either inconel-x, stainless steel, or titanium. With a small degree of error inconel-x, stainless steel and titanium may be used for matching with each other.

Some examples of the possible scale ratios resulting from the use of different materials and utilizing air as a tunnel gas are given in Fig. 4. It is apparent that mutual satisfaction of M, Re, P_∞/E_0, k_∞/K_0 and $\alpha_0 T_0$ is at best only approximate for certain particular model-prototype combinations and even then for scale ratios not very far different from 1. For example, the best combination appears to be a titanium prototype with a stainless steel model at a scale

---

[*] k_∞ and μ_∞ have been replaced here by k_0 and μ_0 since as mentioned above, both these can generally be expressed in the form of Eq. (3.3) in this temperature range.

ratio of 3.4. An aluminum prototype, because of the k_∞/K_0 condition, cannot be simulated by a model constructed of stainless steel, inconel-x or titanium (see Fig. 3).

It should be noted that similitude of thermal stresses and deformations depends on both the temperature distribution $\bar{T}$ and the parameter $\alpha_0 T_0$ as mentioned in section 2. Thus, since simulation of $\bar{T}$ depends on k_∞/K_0, simulation of thermal stresses will depend on k_∞/K_0 as well as on $\alpha_0 T_0$. Furthermore, since the temperature ratio $\bar{T}$ is the same for model and prototype, the initial temperature of the model must be in the same ratio to the prototype initial temperature as $(T_0)_m/(T_0)_p$. Thus if $(T_0)_m$ is less than $(T_0)_p$ it may be necessary to refrigerate the model initially. If the model is of uniform material throughout this presents no problem. However, if various portions of the model are constructed of different materials then stresses may arise as a result of unequal coefficients of expansion of the different materials.

3.2 Use of Gases Other Than Air in the Wind Tunnel

The use of a gas other than air as the test medium provides another approach to the problem of simulating the parameters of the general aerothermoelastic problem.

Helium has received attention as a substitute for air primarily because of its low condensation temperature, eliminating the necessity of heating the wind tunnel gas (Ref. 11). Helium is also attractive because of its high thermal conductivity. A model constructed of either aluminum or magnesium and tested in helium will match the k_∞/K_0 condition with prototypes constructed of inconel-x, stainless steel, or titanium, with much less error than if air were used (Fig. 1). However, if the Mach number, Reynolds number and the ρ_0/E_0 conditions are also to be satisfied simultaneously (Eq. (3.2)), a lower scale ratio L_p/L_m results with helium than with air.

This is due primarily to the lower molecular weight of helium. It may be seen from Eq. (3.2) that a model, made of the same material as the prototype, and tested in a substitute gas, will have a scale ratio L_p/L_m equal to $\frac{\mu_{AIR}}{\mu_{GAS}}\sqrt{\frac{(\sigma^m)_{GAS}}{(\sigma^m)_{AIR}}}$ times the scale ratio of the equivalent test in air at the same Mach number, Reynolds number, temperature, and pressure. Thus the desirable characteristics of a substitute gas are greater molecular weight and lower viscosity than air. Fig. 5, derived from the data of Refs. 12, 13 and 14, presents some properties of gases which have been considered as possible substitutes for air. Regarding scale ratio, helium is the least attractive, providing a scale ratio .38 times that available with air, while $C_4 F_{10}$, the heaviest gas, provides a scale ratio 3.86 times greater than is possible with air under the same tunnel conditions.

The substitute gases of Fig. 5 do not have the same specific heat ratio γ as air. At the higher supersonic speeds, the normal pressure distribution on the lifting surface is dependent on γ and failure to simulate this parameter is one of the primary disadvantages of using a substitute gas. Thus $C_4 F_{10}$ with $\gamma = 1.06$, which was the most attractive from scale ratio considerations, now appears undesirable. Reference 12 shows that a means of simulating γ exactly is possible by properly mixing a heavy monatomic gas, such as argon, krypton or xenon, with a suitable heavy polyatomic gas. Three illustrations of this are also given in Fig. 5, in which $CB_r F_3$, SF_6 and CF_4 are each combined with argon in proportions that yield a γ of 1.4 for the mixture. The improvement in scale ratio, for each of these mixtures, is seen to be approximately 1.5 times greater than is possible for the corresponding test in air.

There are other advantages to be realized by using a heavy gas for aeroelastic testing. At a fixed temperature,

the speed of sound is lower in a heavier gas, consequently, tests conducted at a given Mach number and temperature in a heavy gas will be run at a lower velocity than the corresponding test in air. The advantage of a reduced velocity enables the Froude number U^2/gL to be satisfied, if this is important, for scale ratios other than 1. Also, oscillation frequencies in a flutter test will be reduced, and more important, the horsepower required of the tunnel is only a fraction of that required for air at the same tunnel conditions, (see Ref. 12).

By using a combination of both different gases and different materials at different temperatures, somewhat larger scale ratios can be achieved. Combining the results above with those of section 3.1, scale ratios of approximately $3.4 \times 1.5 \approx 5$ can be roughly achieved.

It has been shown in this section that by using different materials and gases satisfaction of the similarity parameters of the general aerothermoelastic problem is extremely difficult. Where scale ratios other than 1 are possible they are still not very large, and appear inadequate for testing complete wings or wing-body combinations.

4. SPECIALIZATIONS OF AEROTHERMOELASTIC SIMILARITY LAWS

The scaling requirements of the general aerothermo-elastic problem considered in the previous sections have been shown to be very stringent and difficult to satisfy completely. It is possible however, that by considering specific aerother-moelastic problems and hence using more specialized governing equations than the general ones of the previous sections, to arrive at less restrictive similarity conditions. This technique may also help point out the significance of the various general similarity conditions.

4.1 Specialized Aerodynamic Similarity

The boundary layer concept introduced by Prandtl has permitted the solution of aerodynamic flow about an object to be divided into two separate problems; the first dealing with the determination of the pressure distribution, and the second dealing with the determination of the viscous and heating effects in a thin boundary layer region close to the body. This separation appears valid for high Reynolds numbers and for M less than about 5, and is widely used in many circumstances for estimating pressure distribution and heat transfer data.

a) Aerodynamic Pressure Distribution

For determining the pressure distribution about an object, the governing equations are assumed those of a non-viscous, non-heat-conducting fluid. Under these conditions, the viscosity μ and heat conduction k are assumed zero in the general aerodynamic equations (Eqs. (2.1) to (2.5)), and the required similarity reduces to constant values of

$$M, \quad \gamma, \quad \frac{Ut_o}{L}, \quad \bar{\bar{c}}_p, \quad \frac{u_o}{L}, \quad \frac{T_o}{T_\infty} \tag{4.1}$$

The term, u_0/L, arises, as mentioned previously, from the boundary condition of no flow through the body and here requires the ratio of the thickness (and/or displacement) u_0 to the scale length L, to be the same on both model and prototype. The similarity conditions expressed above are far less stringent than those of Eqs. (2.13) chiefly because of the absence of the Reynolds number Re requirement, and indeed are in wide use in determining aerodynamic pressures, stability, and flutter data from wind tunnel models.

In certain circumstances, the similarity conditions of Eq. (4.1) can be reduced still further. For small perturbations in a shockless flow at Mach numbers greater than about 2.5, aerodynamic piston theory (see Ref. 15) can frequently be used to describe the pressure differential between upper and lower surfaces of a thin lifting surface. This can be written in the form,

$$\Delta p = -\frac{4q}{M}\left[1 + \frac{(\gamma+1)}{4} M \frac{d\delta}{dx}\right]\left[\frac{\partial w}{\partial x} + \frac{1}{U}\frac{\partial w}{\partial t}\right] \tag{4.2}$$

where q represents the dynamic pressure, δ represents the thickness of the surface, and w the displacement of the mean line of the surface. Non-dimensionalizing as before, the above reduces to,

$$\frac{\Delta p}{p_0} = -2\gamma\left(M\frac{u_0}{L}\right)\left[1 + \frac{\gamma+1}{4}\left(M\frac{\delta_0}{L}\right)\frac{d\bar{\delta}}{d\bar{x}}\right]\left[\frac{\partial \bar{w}}{\partial \bar{x}} + \left(\frac{L}{Ut_0}\right)\frac{\partial \bar{w}}{\partial \bar{t}}\right] \tag{4.3}$$

The similarity requirements are then simply

$$M\frac{u_0}{L} , \; M\frac{\delta_0}{L} , \; \gamma , \; \frac{Ut_0}{L} , \; \bar{\bar{\delta}} \tag{4.4}$$

It can be seen here that Mach number similarity is no longer required by itself, but rather in the combined parameters $M \frac{u_o}{L}$ and $M \frac{\delta_o}{L}$. If the thickness distribution, $\bar{\delta} = \delta/\delta_o$, and downward deflection distribution $\bar{w} = w/u_o$ are similar, the similarity requirements above can permit different Mach numbers in model and prototype, provided only that both model and prototype are adequately characterized by piston theory.

Aerodynamic similarity relations for the same family of profiles and shapes can likewise be derived in the subsonic, transonic, and low supersonic regimes. These constitute the well known aerodynamic similarity rules (see for example Ref. 16) and are useful in relating the pressure characteristics of similar families of slender bodies.

In considering hypersonic Mach numbers[*] $(M > 5)$, there is an interaction between thickness of the boundary layer and the external flow field which affects the external pressure distribution. This specific similarity problem is discussed in Ref. 17, and it is shown there that an additional combined parameter $M^3/\sqrt{Re}$ should be included in the aerodynamic pressure similarity conditions of Eqs. (4.4) together with Pr, T_∞/T_o, and $\bar{\bar{c}}_p$ requirements.

In the vicinity of noses of blunt bodies at $M = 2.5$, the Mach number disappears altogether from the required similarity parameters, as then Newtonian type flow considerations take over (see Ref. 18). The pressure distribution can then be expressed simply as

$$\frac{p}{p_{stag.}} = \cos^2\theta \tag{4.5}$$

---

[*] This is somewhat greater than the regions here investigated

where θ represents the flow deviation angle at the surface of the body. This is one of the features that makes shock tube investigations at high Mach numbers useful.

b) Viscous and Heating Effects

For obtaining viscous and heating effects, one must look at the complete equations as given by Eqs. (2.1) to (2.5). These can be simplified further through Prandtl's order of magnitude argument, to yield solutions in the boundary layer region close to the body. The required similarity parameters however still remain the same as given by Eq. (2.13) for the most general conditions.

Under certain circumstances, these parameters can be made less restrictive. The unsteady effects associated with heating are generally small, and hence the parameter Ut_0/L can usually be neglected. For the two-dimensional, steady, laminar flow over an isothermal, semi-infinite flat plate, the boundary layer equations can be solved to give the following expression for the heat flux input q_H

$$q_H = \left(k \frac{\partial T}{\partial \eta} \right)_{AIR} = .332 \sqrt{\frac{U \rho}{\mu x}} \left(P_r \right)^{1/3} k \left(T_{AW} - T_W \right) \tag{4.6}$$

where $T_{AW} = T_\infty \left[1 + \frac{\gamma-1}{2} r M^2 \right]$ = adiabatic wall temperature. For thin surfaces with samll pressure gradients the above expression can give a reasonable estimate to the amount of heating experienced by the wing in laminar flow.

Upon non-dimensionalization of Eq. (4.6) one obtains

$$q_H = \left(k \frac{\partial T}{\partial \eta} \right)_{AIR} = \left(\frac{k_0 T_0}{L} \right) . 332 \sqrt{(R_e)} (P_r)^{1/3} \frac{k}{\sqrt{x}} \left(\frac{T_{AW}}{T_0} - T \right) \tag{4.7}$$

The above in combination with the general heat conduction equation at the surface, Eq. (2.19), results (upon neglecting radiation for the present) in the parameters

$$.332 \frac{k_o}{K_o} \sqrt{(R_e)} \, (P_R)^{1/3} \, , \quad \frac{T_{AW}}{T_o} \, , \quad \bar{\bar{k}} \, , \quad \vec{K} \qquad (4.8)$$

The second parameter defines the reference temperature in terms of the adiabatic wall temperature, while the first combined parameter involving Reynolds number does away with a good many of the previous separate aerodynamic and thermal requirements. Thus, the necessity of similar Mach number is not required for viscous heating under these circumstances. (Notice, though, that the coefficient .332 may change somewhat as a function of Mach number, but this can readily be accounted for in the above combined parameter). The presence of temperature gradients on the plate will not affect the above similarity relation if one assumes the validity of the Lighthill approximation to the heat transfer (see Ref. 19).

For turbulent flows over thin surfaces with small pressure gradients, the analogous similarity parameter to the first one of Eq. (4.8) is,

$$.0296 \frac{k_o}{K_o} \, (R_e)^{4/5} (P_r)^{1/3} \qquad (4.9)$$

where now the coefficient .0296 is somewhat more affected by Mach number than in the laminar case. As in the laminar case, the presence of temperature gradients will have very little effect on this similarity parameter (Ref. 20).

The validity of the above similarity parameters can be shown to extend also to the aerodynamic heating at the

noses of blunt bodies providing the constants are altered to
.763 and .042 respectively (Ref. 21). The location of the
transition point from laminar to turbulent flow is however a
nebulous quantity. For certain circumstances however, it may
be assumed to be independent of Mach number to a first ap-
proximation.

To summarize then, it is seen that by means of the
Prandtl boundary layer concept for high Reynolds numbers and
not too high Mach numbers, that it is possible to associate
the pressure distribution similarity mainly with the Mach
number parameter M, and the viscous and heating similarity
mainly with the Reynolds number parameter Re. In certain
circumstances (for example, flow over thin surfaces), it is
possible to relax somewhat the requirement of Mach number
and Reynolds number being individually similar, and to obtain
rather, combined parameters such as Eqs. (4.4) and (4.8)
which can be easier to satisfy. Of course, if in any model
test either pressure distribution or viscous drag and heating
is unimportant, the corresponding similarity parameters may
be neglected without great loss of accuracy for the particular
test.

4.2 Heat Conduction

a) Thin Plates

In the heating of a thin plate, the temperature
tends to rise uniformly across the plate thickness resulting
in a zero temperature gradient in the thickness direction.
Under these conditions the heat conduction equation for a
thin plate of thickness δ may be written as

$$\frac{\partial}{\partial x}\left(\kappa\delta\frac{\partial T}{\partial x}\right) + \frac{\partial}{\partial y}\left(\kappa\delta\frac{\partial T}{\partial y}\right) = \rho_0 C_p \delta\frac{\partial T}{\partial t} - k\left(\frac{\partial T}{\partial z}\right)_{AIR} + \epsilon\sigma T^4 \qquad (4.10)$$

where the last two terms on the right hand side represent
the aerodynamic heating input and radiation heat loss, re-
spectively, over the surface of the plate. The boundary
conditions in this case need only be applied to the edges of
the plate and not to the surface. The conditions for appli-
cability of this thin plate assumption are generally that
the quantity $h\delta/K$ be less than about 1, where h, δ, K are
the heat transfer coefficient, the thickness, and the thermal
conductivity respectively.

Non-dimensionalizing by introducing the same para-
meters as in Section 2 plus the additional thickness distri-
bution parameter $\bar{\delta} = \delta/\delta_0$ results in

$$\frac{\partial}{\partial \bar{x}}\left(\bar{\bar{K}}\,\bar{\delta}\frac{\partial \bar{T}}{\partial \bar{x}}\right) + \frac{\partial}{\partial \bar{y}}\left(\bar{\bar{K}}\,\bar{\delta}\frac{\partial \bar{T}}{\partial \bar{y}}\right) = \left(\frac{L^2}{K_0 t_0}\right)\bar{\bar{C}}_p\,\bar{\delta}\frac{\partial \bar{T}}{\partial \bar{t}} - \left(\frac{k_\infty L}{K_0 \delta_0}\right)\bar{k}\left(\frac{\partial \bar{T}}{\partial \bar{z}}\right)_{AIR}$$

$$+\left(\frac{\epsilon_0 T_0^3 L^2}{K_0 \delta_0}\right)\sigma\bar{\bar{\epsilon}}\,\bar{T}^4 \qquad (4.11)$$

The resulting similarity parameters for the temperature dis-
tribution in the thin plate are then

$$\frac{k_\infty L}{K_0 \delta_0} \quad, \quad \frac{K_0 t_0}{L^2} \quad, \quad \frac{\epsilon_0 T_0^3 L}{k_\infty} \quad, \quad \bar{K}, \bar{\bar{C}}_p, \bar{k}, \bar{\epsilon} \qquad (4.12)$$

The similarity conditions of Eq. (4.12) are less restrictive
than those of Eq. (2.33) since, by using a different material
or gas for the model, the plate thickness δ_0 need not be
scaled in the same manner as the characteristic length L.
This is manifested by the parameter $k_\infty L/K_0 \delta_0$ which replaces
the parameter k_∞/K_0 of Eq. (2.21). The edge boundary con-
ditions will introduce no additional parameters to Eq. (4.12).

If the further assumption of no heat conduction in the x and y directions can be made, the left hand side of Eq. (4.11) is set equal to zero and the non-dimensional parameters become

$$\frac{t_o k_o}{\rho_o C_{P_o} \delta_o L} \quad , \quad \frac{\epsilon_o T_o^3 L}{k_\infty} \quad , \quad \bar{\bar{C}}_P \; , \; \bar{\bar{k}} \; , \; \bar{\bar{\epsilon}} \qquad (4.13)$$

These parameters allow even greater flexibility because there is no scaling restriction on the plate thickness other than the requirement that the model also be thermally thin. The first parameter of Eq. (4.13) will serve only to define the reference time t_o of the thermal response of the plate.

b) Thick Plates

The similarity parameters for the temperature distribution in a thick plate are the same as for the arbitrary body, Eqs. (2.18) and (2.21). However, flexibility in the scaling of the plate thickness is possible for situations where the temperature gradients in the x and y directions are negligible. Non-dimensionalizing the z direction with respect to δ_o instead of L and neglecting the temperature gradients $\frac{\partial T}{\partial x}$, $\frac{\partial T}{\partial y}$, Eqs. (2.15) and (2.19) will yield the parameters,

$$\frac{K_o L}{k_\infty \delta_o} \quad , \quad \frac{K_o t_o}{\delta_o^2} \quad , \quad \frac{\epsilon_o T_o^3 L}{k_\infty} \quad , \quad \bar{\bar{K}} \, , \; \bar{\bar{k}} \, , \; \bar{\bar{C}}_P \, , \; \bar{\bar{\epsilon}} \qquad (4.14)$$

Therefore, as with the thermally thin plate problem, the reference thickness δ_o of a thick plate need not be scaled in the same manner as L if a different material or gas is used for the model.

c) Built-Up Wing Structures

Consider the built-up type of wing of Fig. 6 consisting of several webs and ribs. If the skin is thermally thin, the governing non-dimensional heat conduction equation will be Eq. (4.11). For each web, the non-dimensional heat conduction equation is

$$\frac{\partial}{\partial \bar{y}}\left(\bar{\bar{K}}_w \bar{\bar{\delta}}_w \frac{\partial \bar{T}_w}{\partial \bar{y}}\right) + \frac{\partial}{\partial \bar{z}}\left(\bar{\bar{K}}_w \bar{\bar{\delta}}_w \frac{\partial \bar{T}_w}{\partial \bar{z}}\right) = \left(\frac{L^2}{K_{o_w} t_o}\right) \bar{\bar{C}}_{P_w} \bar{\bar{\delta}}_w \frac{\partial \bar{T}_w}{\partial \bar{t}} \qquad (4.15)$$

and the boundary conditions at each skin-web junction are

$$\bar{T}_s = \bar{T}_w \qquad (4.16a)$$

$$2 \bar{\bar{\delta}}_s \bar{\bar{K}}_s \frac{\partial \bar{T}_s}{\partial \bar{x}} = \left(\frac{\delta_{w_o} K_{w_o}}{\delta_{s_o} K_{s_o}}\right) \bar{\bar{\delta}}_w \bar{\bar{K}}_w \frac{\partial \bar{T}_w}{\partial \bar{z}} \qquad (4.16b)$$

where

$$\bar{\bar{\delta}}_w = \frac{\delta_w}{\delta_{w_o}} \quad , \quad \bar{\bar{K}}_w = \frac{K_w}{K_{w_o}} \quad , \quad \bar{\bar{C}}_{P_w} = \frac{C_{P_w}}{C_{P_{w_o}}} \qquad (4.16c)$$

The resulting non-dimensional parameters from Eqs. (4.11), (4.15) and (4.16), are

$$\frac{k_o L}{K_{o_s} \delta_{o_s}} \quad , \quad \frac{K_{o_s} t_o}{L^2} \quad , \quad \frac{K_{o_w} t_o}{L^2} \quad , \quad \frac{\delta_{w_o} K_{w_o}}{\delta_{s_o} K_{s_o}} \quad , \quad \frac{\epsilon_{o_s} T_o^3 L}{k_o} \quad , \quad \frac{S}{h}$$

$$\bar{\bar{K}}_s \, , \ \bar{\bar{K}}_w \, , \ \bar{\bar{k}} \, , \ \bar{\bar{C}}_{P_s} \, , \ \bar{\bar{C}}_{P_w} \, , \ \bar{\bar{\epsilon}}_s \qquad (4.17)$$

The first two parameters relate to the skin similarity, while the third relates to the web time history. The fourth parameter relates to the junction boundary condition. The parameter S/h requires that model and prototype have the same

internal heat flow paths. Quite often, in regions away from the leading and trailing edges of the wing, conduction along the outer skin is negligible and the terms containing temperature gradients in the x and y directions in Eqs. (4.11), (4.15) and (4.16) may be neglected. Therefore, the parameters of Eq. (4.13) will apply for the skin and the similarity parameters for the skin-web combination become

$$\frac{t_o k_\infty}{\rho_s C_{P_{0s}} \delta_{0s} L} \quad , \quad \frac{K_{ow} t_o}{L^2} \quad , \quad \frac{\epsilon_{os} T_o^3 L}{k_\infty} \quad , \quad \frac{S}{h}$$

$$\overline{\overline{K_w}} \quad , \quad \overline{\overline{k}} \quad , \quad \overline{\overline{C_{P_s}}} \quad , \quad \overline{\overline{C_{P_w}}} \quad \overline{\overline{\epsilon_s}}$$

(4.18)

The first parameter of Eq. (4.18) may be combined with the second to give the alternate parameter $\left(\frac{K_{ow}}{K_{os}}\right) \cdot \left(\frac{\delta_s k_s}{L k_\infty}\right)$. Hence Eq. (4.18) may also be written as

$$\left(\frac{K_{ow}}{K_{os}}\right) \cdot \left(\frac{\delta_{os} k_{os}}{L k_\infty}\right) \quad , \quad \frac{K_{ov} t_o}{L^2} \quad , \quad \frac{\epsilon_{os} T_o^3 L}{k_\infty} \quad , \quad \frac{S}{h}$$

$$\overline{\overline{K_w}} \quad , \quad \overline{\overline{k}} \quad , \quad \overline{\overline{C_{P_s}}} \quad , \quad \overline{\overline{C_{P_w}}} \quad , \quad \overline{\overline{\epsilon_s}}$$

(4.19)

Therefore, it is seen that with the assumption of zero temperature gradients in the x and y directions in a thermally thin skin, the parameters of Eq. (4.17) are considerably reduced.

If both skins and webs are thick the similarity parameters that will generally apply are Eqs. (2.18) and (2.21) and it is necessary to have a model which is a geometrically scaled replica of the prototype. However, if temperature gradients across the thickness of the web are negligible, the

web thickness need not be scaled in the same manner as L if the skins and webs are not of the same materials. This is possible because of the parameter $\frac{\delta_{wo}\ K_{wo}}{\delta_{so}\ K_{so}}$ of Eq. (4.17) which results from the skin-web junction boundary condition and allows one to use different materials for the model and prototype.

Still simpler similarity relations can be obtained for these built-up wing structures if one is willing to make certain assumptions regarding the heating-up process. During the early period of this heating process, while the skin is heating up, very little heat is conducted into the web and the web remains essentially at its initial temperature. (This assumption is further justified by any joint resistance at the skin-web junction). Hence, the web will introduce no similarity parameters during this early period. This situation is applicable if the skin is either thick or thin, and is important because during these early times, the temperature differences between skin and web may become large and the resulting thermal stresses may be appreciable. The thermal similarity requirements will then be Eqs. (4.12), (4.13) or (4.14) of the immediately preceding sections a) or b).

At some later time, it may be assumed that the skins have heated up to close to their steady state equilibrium temperature while the webs have remained essentially at their initial temperature. Then, after this time, heat will be conducted to the webs and the skin temperature may be regarded as a boundary condition at the skin-web junction. This assumption is again more valid if there is any thermal resistance at the skin-web junction. The similarity parameters for this situation at these later times are those required for simulation of the steady state temperature of the thin skin and Eqs. (4.15) and (4.16a) for the web

$$\frac{t_0 K_{ow}}{L^2} \;,\quad \frac{E_{os} T_0 L^3}{k_o} \;,\quad \bar{K}_w,\; \bar{k},\; \bar{C}_{P_w},\; \bar{E}_s,\; \frac{S}{h} \qquad (4.20)$$

4.3 Stresses and Deflections of Equivalent Plates

The structural behavior of plates constitutes an increasingly important region of structural analysis of aircraft. Low aspect ratio wings are characteristically thin and deform much like a plate. A convenient means of representing a wing of this type is to transform the actual structure into an equivalent plate of varying bending and extensional stiffnesses. The similarity requirements under the combined effects of heating and aerodynamic loading may then be derived from the plate equations.

The governing differential equations of a heated isotropic plate are,

$$\frac{\partial^2}{\partial x^2}\left[D\left(\frac{\partial^2 w}{\partial x^2} + \nu\frac{\partial^2 w}{\partial y^2}\right)\right] + \frac{\partial^2}{\partial y^2}\left[D\left(\frac{\partial^2 w}{\partial y^2} + \nu\frac{\partial^2 w}{\partial x^2}\right)\right] + 2\frac{\partial^2}{\partial x \partial y}\left[D(1-\nu)\frac{\partial^2 w}{\partial x \partial y}\right] =$$

$$p(x,y,t) + \frac{\partial^2 F}{\partial y^2}\frac{\partial^2 w}{\partial x^2} + \frac{\partial^2 F}{\partial x^2}\frac{\partial^2 w}{\partial y^2} + 2\frac{\partial^2 F}{\partial x \partial y}\frac{\partial^2 w}{\partial x \partial y} - \frac{\partial^2 M_T}{\partial x^2} - \frac{\partial^2 M_T}{\partial y^2} \qquad (4.21)$$

$$\frac{\partial^2}{\partial x^2}\left[\frac{1}{C(1-\nu^2)}\left(\frac{\partial^2 F}{\partial x^2} - \nu\frac{\partial^2 F}{\partial y^2}\right)\right] + \frac{\partial^2}{\partial y^2}\left[\frac{1}{C(1-\nu^2)}\left(\frac{\partial^2 F}{\partial y^2} - \nu\frac{\partial^2 F}{\partial x^2}\right)\right] + 2\frac{\partial^2}{\partial x \partial y}\left[\frac{1}{C(1-\nu)}\frac{\partial^2 F}{\partial x \partial y}\right] =$$

$$\left(\frac{\partial^2 w}{\partial x \partial y}\right)^2 - \frac{\partial^2 w}{\partial x^2}\frac{\partial^2 w}{\partial y^2} - \frac{\partial^2}{\partial x^2}\left[\frac{N_T}{C(1+\nu)}\right] - \frac{\partial^2}{\partial y^2}\left[\frac{N_T}{C(1+\nu)}\right] \qquad (4.22)$$

where $p(x,y,t)$ is the distributed loading per unit area.

These two equations are the Von Kármán equations for large deflections of a plate with variable stiffness properties under applied loads and thermal stresses. The quantity $w(x,y,t)$ is the lateral deflection of the neutral surface from its initial position, F is the stress function, C and D are the extensional and bending stiffnesses per unit length respectively, and N_T and M_T are the midplane thermal force and moment per unit length, respectively. These latter four quantities are defined generally by

$$C = \int_{-\frac{h}{2}}^{\frac{h}{2}} \frac{E}{1-\nu^2} \, dz \quad , \quad D = \int_{-\frac{h}{2}}^{\frac{h}{2}} \frac{E z^2}{1-\nu^2} \, dz$$

$$N_T = \int_{-\frac{h}{2}}^{\frac{h}{2}} \frac{E \alpha \Delta T}{1-\nu} \, dz \quad , \quad M_T = \int_{-\frac{h}{2}}^{\frac{h}{2}} \frac{E \alpha \Delta T z}{1-\nu} \, dz \tag{4.23}$$

where E is the modulus of elasticity, α the coefficient of thermal expansion, ν Poisson's ratio, and ΔT the temperature rise from some initial value and h is the plate depth. The lateral loading p may be due to the combined effects of aerodynamic, inertial, and gravity forces. As discussed in Section 4.1a), at supersonic Mach numbers greater than about 2.5, the aerodynamic pressure loading p_A may be determined by piston theory, Eq. (4.2), which has the equivalent form

$$p_A = -2 \gamma p_o M \left[1 + \frac{(\gamma+1)}{4} M \frac{\partial h}{\partial x} \right] \left[\frac{\partial w}{\partial x} + \frac{1}{U} \frac{\partial w}{\partial t} \right] \tag{4.24}$$

The displacement $w(x,y,t)$ will in general include rigid body displacements as well as elastic deformations. If the rigid body displacements of vertical translation and pitching are considered, the following equations of equilibrium must also be satisfied in addition to Eqs. (4.21) and (4.22)

$$-\iint_S m\left(\frac{\partial^2 w}{\partial t^2}+g\right)dx\,dy + \iint_S p_A\,dx\,dy = 0$$

$$-\iint_S m\left(\frac{\partial^2 w}{\partial t^2}+g\right)x\,dx\,dy + \iint_S p_A\,x\,dx\,dy = 0$$

(4.25)

where m is the airplane mass density per unit area. Introducing the following non-dimensional parameters

$$\bar{w} = w/u_0 \quad , \quad \bar{x} = x/L \quad , \quad \bar{y} = y/L \quad , \quad \bar{h} = h/h_0$$

$$\bar{t} = t/t_0 \quad , \quad \bar{F} = F/C_0 L^2 \quad , \quad \bar{C} = C/C_0 \quad , \quad \bar{D} = D/D_0$$

$$\bar{N}_T = N_T/N_{T_0} \quad , \quad \bar{M}_T = M_T/M_{T_0} \quad , \quad \bar{m} = m/m_0$$

(4.26)

Eqs. (4.21) and (4.22) in non-dimensional form become

$$\frac{\partial^2}{\partial \bar{x}^2}\left[\bar{D}\left(\frac{\partial^2 \bar{w}}{\partial \bar{x}^2}+\nu\frac{\partial^2 \bar{w}}{\partial \bar{y}^2}\right)\right] + \frac{\partial^2}{\partial \bar{y}^2}\left[\bar{D}\left(\frac{\partial^2 \bar{w}}{\partial \bar{y}^2}+\nu\frac{\partial^2 \bar{w}}{\partial \bar{x}^2}\right)\right] + 2\left[\bar{D}(1-\nu)\frac{\partial^2 \bar{w}}{\partial \bar{x}\,\partial \bar{y}}\right] =$$

$$-2\left(\frac{\gamma\rho_0 M L^3}{D_0}\right)\left[1+\frac{(\gamma+1)}{4}(M\frac{h_0}{L})\frac{\partial \bar{h}}{\partial \bar{x}}\right]\left[\frac{\partial \bar{w}}{\partial \bar{x}}+\left(\frac{L}{u_0 t_0}\right)\frac{\partial \bar{w}}{\partial \bar{t}}\right] - \left(\frac{m_0 L^4}{D_0 t_0^2}\right)\bar{m}\frac{\partial^2 \bar{w}}{\partial \bar{t}^2}$$

(4.27)

$$-\left(\frac{m_0 g L^4}{u_0 D_0}\right)\bar{m} + \left(\frac{C_0 L^2}{D_0}\right)\left[\frac{\partial^2 \bar{F}}{\partial \bar{y}^2}\frac{\partial^2 \bar{w}}{\partial \bar{x}^2} + \frac{\partial^2 \bar{F}}{\partial \bar{x}^2}\frac{\partial^2 \bar{w}}{\partial \bar{y}^2} + 2\frac{\partial^2 \bar{F}}{\partial \bar{x}\,\partial \bar{y}}\frac{\partial^2 \bar{w}}{\partial \bar{x}\,\partial \bar{y}}\right]$$

$$-\left(\frac{L^2 M_{T_0}}{u_0 D_0}\right)\left[\frac{\partial^2 \bar{M}_T}{\partial \bar{x}^2}+\frac{\partial^2 \bar{M}_T}{\partial \bar{y}^2}\right]$$

$$\frac{\partial^2}{\partial \bar{x}^2}\left[\frac{1}{\bar{\bar{C}}(1-\nu^2)}\left(\frac{\partial^2 \bar{F}}{\partial \bar{x}^2} - \nu \frac{\partial^2 \bar{F}}{\partial \bar{y}^2}\right)\right] + \frac{\partial^2}{\partial \bar{y}^2}\left[\frac{1}{\bar{\bar{C}}(1-\nu^2)}\left(\frac{\partial^2 \bar{F}}{\partial \bar{y}^2} - \nu \frac{\partial^2 \bar{F}}{\partial \bar{x}^2}\right)\right]$$

$$+ 2\frac{\partial^2}{\partial \bar{x}\partial \bar{y}}\left[\frac{1}{\bar{\bar{C}}(1-\nu)}\frac{\partial^2 \bar{F}}{\partial \bar{x}\partial \bar{y}}\right] = \left(\frac{U_0}{L}\right)^2\left[\left(\frac{\partial^2 \bar{w}}{\partial \bar{x}\partial \bar{y}}\right)^2 - \frac{\partial^2 \bar{w}}{\partial \bar{x}^2}\frac{\partial^2 \bar{w}}{\partial \bar{y}^2}\right]$$

$$\quad (4.28)$$

$$-\left(\frac{N_{T_0}}{C_0}\right)\left[\frac{\partial^2}{\partial \bar{x}^2}\left(\frac{\bar{\bar{N}}_T}{\bar{\bar{C}}(1+\nu)}\right) + \frac{\partial^2}{\partial \bar{y}^2}\left(\frac{\bar{\bar{N}}_T}{\bar{\bar{C}}(1+\nu)}\right)\right]$$

The resulting non-dimensional parameters are

$$\frac{\gamma p_0 M L^3}{D_0} \quad , \quad \frac{(\gamma+1)M h_c}{L} \quad , \quad \frac{U t_0}{L} \quad , \quad \frac{m_0 L^4}{D_0 t_0^2} \quad , \quad \frac{m_0 L^4 g}{D_0 u_0} \quad , \quad \frac{U_0}{L}$$

$$\quad (4.29)$$

$$\frac{C_0 L^2}{D_0} \quad , \quad \frac{N_{T_0}}{C_0} \quad , \quad \frac{L^2 M_{T_0}}{u_0 D_0} \quad , \quad \bar{\bar{C}}, \bar{D}, \bar{\bar{M}}_T, \bar{\bar{N}}_T, \bar{\bar{m}}, \bar{h}, \nu$$

The first parameter is the ratio of aerodynamic forces to
bending stiffness and is less restrictive than the P_0/E_0
parameter of Eq. (2.35) since D_0 can be varied by changing
the structural geometry. Also M and γ can be different.
The second condition reflects the aerodynamic thickness effect
as expressed by piston theory and replaces the requirement
that M must be simulated by itself. The third parameter is
the unsteady time parameter of the external flow, the fourth

is the ratio of inertial loading to bending stiffness and
replaces the $\rho_0 u_0 L / \sigma_0 t_0^2$ parameter of Eq. (2.34), the fifth is
the ratio of gravity forces to bending stiffness. The para-
meter u_0/L requires the neutral surface to deflect both simi-
larly and in scale. However, if the elastic deformations are
small such that the non-linear terms in $\bar{w}$ of Eq. (4.28) are
negligible, the u_0/L requirement vanishes. The seventh con-
dition arises from the buckling characteristics of the wing,
the eight and ninth relate to the thermal force and moment
and together replace the $\alpha_0 T_0 L / u_0$ parameter of Eq. (2.34).
Finally, the double-barred quantities are the distributions
of stiffnesses, thermal forces and moments, mass, and external
shape of the wing. No additional parameters will be intro-
duced by the non-dimensional forms of Eq. (4.25).

By suitable combination with $\gamma P_\infty M L^3 / D_0$, $U t_0 / L$,
and the perfect gas relationship $a^2 = \gamma P / \rho$, the parameter
$m_0 L^4 / D_0 t_0^2$ may be rearranged into the alternate more familiar
mass density ratio $1/M (P_\infty L / m_0 g)$. Similarly, the parameter
$m_0 L^4 g / D_0 u_0$ may be changed by combination with $\gamma P_\infty M L^3 / D_0$ and
the above $1/M (P_\infty L / m_0)$ to yield $(u_0/L)(U^2/g L)$. Using these alter-
nate forms, the similarity requirements for the equivalent
plate aeroelastic problem, Eq. (4.29), can be expressed as

$$\frac{\gamma P_\infty M L^3}{D_0} \ , \ \frac{(\gamma+1) M h_0}{L} \ , \ \frac{U t_0}{L} \ , \ \frac{1}{M}\left(\frac{P_\infty L}{m_0}\right) \ , \ \frac{u_0}{L}\left(\frac{U^2}{g L}\right)$$

$$\frac{u_0}{L} \ , \ \frac{C_0 L^2}{D_0} \ , \ \frac{N_{T_0}}{C_0} \ , \ \frac{L^2 M_{T_0}}{u_0 D_0} \ , \ \bar{\bar{C}}, \bar{\bar{D}}, \bar{\bar{M}}_T, \bar{\bar{N}}_T, \bar{\bar{m}}, \bar{h}, \nu \qquad (4.30)$$

The first parameter, in combination with $a^2 = \gamma P_\infty / \rho_\infty$, may take
the alternate form $q L^3/M D_0$ where q is the free stream dynamic
pressure $\frac{1}{2} \rho_\infty U^2$. These specialized parameters are to be
compared with the more general ones of Eq. (2.35).

It should be noted that the parameter U^2/gL is the familiar Froude number and requires the gravitational force to be scaled correctly. This Froude number serves mainly to define the static equilibrium position of the model under its own weight and to determine the equilibrium angle of attack in flying models. Since these are generally not too significant in most aeroelastic testing, the Froude number requirement can be disregarded (see Ref. 22).

The parameters of Eq. (4.30) are also the requirements for flutter similarity. The third condition, Ut_o/L, serves only to define the reference time t_o of the problem. If sinusoidal motion $\overline{w} = \tilde{w} e^{i\omega t_o \bar{t}}$ is assumed as in flutter, the reference time t_o can be associated with the period $1/\omega$, and this similarity parameter becomes the familiar reduced frequency $\omega L/U$. The similarity requirements for flutter without any in-plane stresses (such as due to axial loads, large deflections or aerodynamic heating) reduce mainly to the first five parameters of Eq. (4.30) and also $\overline{D}, \overline{\overline{m}}, \overline{h}, \nu$.

The conditions for static aerothermoelastic similarity are determined by neglecting the parameters Ut_o/L and $m_o L^4/D_o t_o^2$ in Eq. (4.29). Comparison of these resulting static similarity parameters with those of the dynamic case, Eq. (4.30), indicates the absence in Eq. (4.30) of the Ut_o/L parameter, the density ratio parameter $(1/M)(\rho_o L/m_o)$ and the replacing of the Froude number parameter by $m_o L^4/D_o U_o$.

The similarity parameters for a vibration model are obtained by putting the aerodynamic loading f_A equal to zero, i.e., the first three parameters of Eq. (4.29) will be absent. For this situation the important parameters relate to the inertial forces and elastic restoring forces of the wing and simulation of the external flow, except as it affects the heating rate from the boundary layer, is not necessary.

The $m_0 L^4/D_0 t_0^2$ parameter now serves to define the reference time t_0 of the problem. For sinusoidal motion $\bar{w} = \tilde{w} e^{i\omega t_0 \bar{t}}$ of the vibration, this time t_0 can be associated with the period $1/\omega$ and the similarity parameters can be rewritten as

$$\frac{m_0 L^4 \omega^2}{D_0}, \quad \frac{u_0 \omega^2}{g}, \quad \frac{u_0}{L}, \quad \frac{C_0 L^2}{D_0}, \quad \frac{N_{T_0}}{C_0}, \quad \frac{L^2 M_{T_0}}{u_0 D_0}$$

$$\bar{\bar{C}}, \quad \bar{\bar{D}}, \quad \bar{\bar{M}}_T, \quad \bar{\bar{N}}_T, \quad \bar{\bar{\bar{m}}} \tag{4.31}$$

where the parameter $u_0 \omega^2/g$ is the ratio of inertial forces to gravitational forces. The model, under the conditions of Eq. (4.31), will have the same non-dimensional mode shapes at the same non-dimensional frequencies $m_0 L^4 \omega^2/D_0$ as the prototype wing.

4.4 Applications to Panel Flutter and Buckling

The stability of a thin skin panel subjected to aerodynamic heating and aerodynamic pressures on one side is a problem of current interest. The similarity parameters for the study of the self excited oscillations and buckling behavior of the panel may be derived from section 4.3 by properly modifying Eqs. (4.27) and (4.28).

Consider a thin isotropic plate of constant thickness δ with a uniform temperature distribution across the thickness. The quantities C, D, N_T, M_T of Eq. (4.23) become for this plate

$$C = \frac{E\delta}{1-\nu^2}, \quad D = \frac{E\delta^3}{12(1-\nu^2)}, \quad N_T = \frac{E\alpha\Delta T\delta}{1-\nu}, \quad M_T = 0 \tag{4.32}$$

The loading term in Eq. (4.27) will be modified by noting that the aerodynamic thickness term $M h_0/L$ and the gravitational

loading are zero. The non-dimensional parameters for the large deflection behavior of the panel may then be taken from Eq. (4.30) and reduce to

$$\frac{\gamma \rho_\infty M}{E_o} \left(\frac{L}{\delta}\right)^3, \ \frac{Ut_o}{L}, \ \frac{1}{M}\left(\frac{\rho_\infty L}{m_o}\right), \ \frac{u_o}{L}, \ \frac{L}{\delta}, \ (\alpha \Delta T)_o, \ \nu \qquad (4.33)$$

It should be noted again that the first parameter may have the alternate form $(\frac{\gamma}{ME_o})\cdot(\frac{L}{\delta})^3$ and the parameter Ut_o/L serves only to define the reference time t_o of the flow. The boundary conditions along the edges of the plate will introduce no additional parameters to Eq. (4.33). The quantities $\bar{\bar{C}}$, $\bar{\bar{D}}$, $\bar{\bar{N}}_T$ are automatically the same for model and prototype if the same materials and same temperatures are used for both.

It has been shown in Ref. 23 by Hedgepeth that for cases where M is greater than 1.6 and the mass density ratio $m_o/\rho_\infty L$ is greater than 10 (satisfied by most conventional panels), the aerodynamic damping term $m_o/\rho_\infty L$ may be neglected. This permits a reduction in the parameters of Eq. (4.33) because for this situation the parameter $(1/M)(\rho_\infty L/m_o)$ drops out, and the parameter Ut_o/L, is replaced by $m_o L^4/E_o \delta^3 t_o^2$ which will serve to determine the time scale.

For the study of the flutter behavior of a panel which has already buckled, e.g., because of thermal stresses, it is necessary to simulate the large deflections of the plate. However, small deflection theory may be adequate in predicting the onset of flutter of an unbuckled plate. The assumption of small deflections will uncouple Eqs. (4.27) and (4.28) and the stress function $\bar{F}$ may be solved for from Eq. (4.28) in the form

$$\bar{F} = \frac{N_{T_o}}{C_o} g(\bar{x}, \bar{y}) = (\alpha \Delta T)_o g(\bar{x}, \bar{y}) \qquad (4.34)$$

where $g(\bar{x}, \bar{y})$ is a function of $\bar{x}$ and $\bar{y}$ and depends on the boundary conditions. Substitution of $\bar{F}$ into Eq. (4.27) results in the parameter $(\alpha \Delta T)_o$ being replaced by $(L/\delta)^2 (\alpha \Delta T)_o$. Therefore, the small deflection assumption removes the requirement that $(\alpha \Delta T)_o$ and L/δ must be simulated independently and replaces them with the single requirement $(L/\delta)^2 (\alpha \Delta T)_o$.

The similarity requirements for the buckling of a panel by thermal stresses in the absence of aerodynamic and inertial loads may be taken from Eq. (4.33) by neglecting the first three parameters. For this static problem and for large deflections the similarity requirements are

$$\frac{u_o}{L} \quad , \quad \frac{L}{\delta} \quad , \quad (\alpha \Delta T)_o \quad , \quad \nu \tag{4.35}$$

If in addition there is a side loading P_s, such as a constant internal pressure, the following parameter must also be simulated in addition to Eq. (4.35)

$$\frac{P_s L^3}{D} = \frac{P_s}{E_o} \left(\frac{L}{\delta}\right)^3 \tag{4.36}$$

For this buckling case, small deflection theory may be adequate in predicting the onset of buckling, and the parameters L/δ and $(\alpha \Delta T)_o$ need not be simulated independently but in the combined parameter $(L/\delta)^2 (\alpha \Delta T)_o$.

4.5 Application to Low Aspect-Ratio Multi-Web Wing

The parameters derived for the specialized aerothermoelastic situations can also be applied to the low aspect-ratio wing of Fig. 6. For simplicity, assume the ribs and webs are equally spaced a distance S apart, the wing is of uniform material throughout, and the skin and web thick-

nesses are constant. An investigation of similarity under such conditions has been considered by L. Ting in Ref. 5, and serves as an illustration of what can be done with specialized similarity cases.

For this low aspect ratio wing under the above assumptions, the quantities defined in Eq. (4.23) become

$$ C \approx 2 \frac{E \delta_s}{1-\nu^2} \left[1 + \frac{1}{2} \left(\frac{h}{S} \frac{\delta_w}{\delta_s} \right) \right] , \quad D \approx \frac{E h^2 \delta_s}{2(1-\nu^2)} \left[1 + \frac{1}{6} \left(\frac{h}{S} \frac{\delta_w}{\delta_s} \right) \right] $$

$$ N_T \approx \frac{E \alpha T_o \delta_s}{1-\nu} \left[\Delta \overline{T_u} + \Delta \overline{T_L} + \left(\frac{\delta_w h}{\delta_s S} \right) \int_{-\frac{1}{2}}^{\frac{1}{2}} \Delta \overline{T_w} \, d\left(\frac{z}{h} \right) \right] \tag{4.37} $$

$$ M_T \approx \frac{E \alpha T_o h \delta_s}{1-\nu} \left[\frac{\Delta \overline{T_u} - \Delta \overline{T_L}}{2} + \left(\frac{\delta_w h}{\delta_s S} \right) \int_{-\frac{1}{2}}^{\frac{1}{2}} \Delta \overline{T_w} \left(\frac{z}{h} \right) d\left(\frac{z}{h} \right) \right] $$

Assume now that the same materials and same gas are used for both model and prototype, and that the same temperatures exist throughout the model and prototype at corresponding instants of time.[*] Letting C_o, D_o, N_{T_o}, M_{T_o}, denote the quantities of Eq. (4.37) evaluated at some reference cross-sectional thickness $h = h_o$, the similarity conditions for dynamic aerothermoelastic phenomena, Eq. (4.30), reduce to

$$ \frac{\rho_o L^3}{\delta_s h_o^2} , \quad M, \quad \frac{U t_o}{L} , \quad \frac{\rho_o L}{m_o} , \quad \frac{U^2}{g L} $$

---

[*] These assumptions on the temperature distribution will be re-examined later.

$$\frac{u_o}{L} \quad , \quad \frac{h_o}{L} \quad , \quad \frac{\delta_w \, h_o}{\delta_s \, S} \quad , \quad \frac{h_i}{h_o} \tag{4.38}$$

Utilizing the 1st, 7th, and 8th conditions, the following relations between the geometry of the model and prototype can be arrived at,

$$(h_o)_m = \frac{1}{n} \, (h_o)_p$$

$$(\delta_s)_m = \frac{1}{n} \, \frac{(p_\infty)_m}{(p_\infty)_p} \, (\delta_s)_p \tag{4.39}$$

$$(\delta_w)_m = n \, \frac{(\delta_s)_m}{(\delta_s)_p} \, \frac{S_M}{S_P} \, (\delta_w)_p$$

where n is the scale ratio L_P/L_M.

It can be seen from the above relations, that if one is willing to distort the model construction in the scaling down process, a pressure ratio $(p_\infty)_m \big/ (p_\infty)_p$ other than unity can be accomodated.

Turning now to the general aerodynamic similarity, Section 2, it was seen desirable to reproduce the Reynolds number Re as well as the Mach number M in the flow. With Reynolds number and Mach number simulated, the model free stream pressure and density are scaled as follows

$$(p_\infty)_m = n \, (p_\infty)_p \quad , \quad (\rho_\infty)_m = n (\rho_\infty)_p \tag{4.40}$$

This pressure ratio, together with an additional similarity parameter δ_s/S introduced to provide for similar

local buckling characteristics of the upper and lower skin surfaces (see Section 4.4, and also Ref. 5), reduce the relations between model and prototype geometry, Eqs. (4.39) to,

$$(h_0)_m = \frac{1}{n} (h_0)_p$$
$$(\delta_s)_m = (\delta_s)_p$$
$$(\delta_w)_m = n (\delta_w)_p \qquad\qquad (4.41)$$
$$S_M = S_P$$

A model so constructed would satisfy the aerodynamic similarity requirements of Re and M and also the conditions of Eq. (4.30). A look at the remaining similarity conditions is in order.

The mass per unit area of the structure shown in Fig. 6 is

$$m = 2 \rho_B \delta_s \left[1 + \frac{h \delta_w}{s \delta_s} \right] \qquad\qquad (4.42)$$

where ρ_B is the density of the material. Substituting this into the mass density ratio $\rho_\infty L / m_0$ condition gives

$$\frac{\rho_\infty L}{\rho_B \delta_s \left[1 + \frac{h_0 \delta_w}{s \delta_s} \right]} \qquad\qquad (4.43)$$

which will be the same for model and prototype if $(\rho_B)_m = (\rho_B)_p$, i.e., similar materials for both. This insures similar dynamic aeroelasticity properties.

The $U t_0 / L$ parameter, as mentioned previously, serves to define the dimensionless time t_0 associated with dynamic problems and does not present a problem in simulation here.

The u_0/L parameter serves to define the reference deflection u_0 and indicates that deflections will be in the same scale as the model scale ratio n.

The h/h_0 parameter requires that the thickness distribution of model and prototype be similar.

The Froude number parameter V^2/gL will not be satisfied under the foregoing conditions unless the scale ratio n is equal to 1. However, as mentioned previously, the requirement for Froude number is not too significant in most aeroelastic testing and can be usually disregarded.

The question of the heat conduction similarity must now also be considered in connection with the original assumption of the same temperatures existing throughout both model and prototype at corresponding instants of time. Because the model's dimensions have been distorted from those of the prototype according to Eqs. (4.41), no unique correspondence in temperature distribution exists at all periods of time. However, under the simplifying assumptions in the character of the heat flow as discussed at the end of Section 4.2c), a rough correspondence in the temperature distributions can be determined for either very early times or very late times. Thus, at very early times, it may sometimes be adequate to assume that while the thin skin is heating up, there is no heat conduction into the web and that the web remains essentially at zero initial temperature (this assumption is further justified by any joint resistance at the skin-web intersection). Also, it can be assumed that there is negligible heat conduction along the skin. It can then be shown that the reference time for this distorted model at early times is related to that of the prototype by, (see Eq. (4.13))

$$(t_0)_M = \frac{1}{n} (t_0)_P \qquad (4.44)$$

This early time assumption may be sufficient to cover the case where the maximum thermal stresses are developed.

Alternatively, for later times, it might be assumed that the thin skins have heated up to the steady state equilibrium temperature value, and that the heat is then conducted into the web according to Eq. (4.15) subject to the boundary condition of constant temperature at the web-skin junction. The corresponding reference times at these later times are then related by (see Eq. (4.20))

$$(t_o)_M = \frac{1}{n^2}(t_o)_P$$

(4.45)

Section 4.5 has served as an illustration of what can be done in the way of satisfying specialized similarity laws for an equivalent plate rather than the most general ones developed in Section 2. By distorting the geometry of the model construction, it has been possible to satisfy both the M and Re criteria. However, the heat conduction similarity is only approximate and contingent on certain assumptions in the heat flow behavior. In view of these latter approximations, it will be shown later in Section 5, that it is probably much more expedient to relax the Re requirement itself, rather than to go to all the trouble of geometrically distorting the model as described here.

5. REYNOLDS NUMBER RELAXATION

The previous sections have discussed the problem
of satisfying the similarity conditions by considering the
use of different materials and gases, and by determining
less restrictive parameters by looking at specialized situa-
tions. As mentioned in Section 2.4, a third means, that of
relaxing one of the conflicting requirements of M, Re, or
ρ_o/E_o is also possible. The ρ_o/E_o requirement is essential
to any aeroelastic type model test, although it can be made
somewhat less restrictive by consideration of specialized
geometries such as equivalent plates; see Eqs. (4.30). The
Mach number M requirement seems fundamental to most compres-
sible flow studies; however, it too can be made somewhat less
restrictive by combination with other parameters for certain
type flows as indicated in Section 4.1a) and by Eq. (4.30).
This relaxing of M has been suggested in Ref. 10 for certain
tests. The relaxation of the difficult Reynolds number Re
requirement, is also possible and appears the most fruitful
in attaining large scale ratios. As previously mentioned
this is often the practice in "cold" aeroelastic testing,
provided a certain minimum Reynolds number is attained. In
this "cold" case, simulation of the Reynolds number is pri-
marily for the purpose of simulating air loads. In the pres-
ent problem, the Reynolds number also influences the rate of
heat transfer from the boundary layer into the structure and
thus serves generally to define the characteristic time of
the heat flow process. Eq. (4.7) shows how the rate of heat
transfer may be approximately related to the Reynolds number.
Thus the importance of simulating the Reynolds number may be
found by investigating the effect of the heat transfer coef-
ficient $h = q_w/(T_{aw}-T_w)$ on particular aerothermoelastic phenomena.

An important effect of aerodynamic heating on aero-
elastic type models are the resulting thermal stresses in the

structure which can subsequently cause reduction in the tor-
sional rigidity of the wing. This loss in torsional rigidity
results from thermally induced compressive axial stresses in
the leading and trailing edges and may affect the structural
integrity of the wing, particularly from flutter considera-
tions. The problem of simulating the temperatures, thermal
stresses and resulting loss in torsional rigidity due to
these stresses, without simulating the Reynolds number, will
now be examined for some particular wing cross sections.

Consider first a two-dimensional solid double wedge
airfoil accelerated instantaneously from M_O to a final Mach
number M_f at constant altitude. This instantaneous accelera-
tion results in the greatest reduction in torsional rigidity
and also is the type of test envisioned for aerothermoelastic
testing. This problem has been studied by Budiansky and
Mayers in Ref. 24 which derives the following expression for
the effective torsional stiffness of the airfoil

$$\frac{GJ_{eff}}{GJ_o} = 1 + \frac{\int_A \sigma_y r^2 dA}{GJ_o} \qquad (5.1)$$

where GJ_o is the initial St. Venant torsional stiffness, σ_y
the axial stress, negative if compressive, r the distance
from the center of twist, and the integral is to be taken
over the cross sectional area A. The temperature in the wing
was determined by assuming one-dimensional heat flow through
the wing thickness, no conduction in the chordwise direction
and constant material properties. At any point along the
wing the temperature T is given by Ref. 24 as

$$\frac{T - T_{AW}^{(o)}}{\Delta T_{AW}} = 1 - e^{-\frac{\lambda}{\delta/\delta_o}} \qquad (5.2)$$

where $T_{AW}^{(o)}$ is the adiabatic wall temperature corresponding to M_o, $\Delta T_{AW} = T_{AW}^{(o)} - T_{AW}^{(f)}$, δ_o is the maximum thickness and λ is the time parameter defined by

$$\lambda = \frac{2 \, h(x) \, t}{\rho_B \, C_{P_B} \, \delta_o} \tag{5.3}$$

The quantities ρ_B and C_{PB} are the material density and specific heat, respectively and t is the physical time. The heat transfer coefficient h(x) may vary along the chord but is not a function of time since altitude and Mach number are constant. It should be noted that the parameter λ corresponds to the parameter $h \, t_o / \rho_B \, C_B \, \delta_o L$ of Eq. (4.13) for temperature similarity in a thermally thin plate.* The in-plane thermal stresses, derived on the basis of elementary theory, have the form

$$\sigma_y = E \alpha \, \Delta T_{AW} \, f\left(\lambda, \frac{x}{c}\right) \tag{5.4}$$

where x is measured along the chord c. With the use of Eqs. (5.2) and (5.4), the effective torsional stiffness, Eq. (5.1), has the form

$$\frac{GJ_{eff}}{GJ_o} = 1 - \frac{E\alpha}{G} \frac{\Delta T_{AW}}{(\delta_o/c)^2} \Delta(\lambda) \tag{5.5}$$

---

* The correspondence is more apparent upon the substitution of h(x) from Eq. (4.7) into Eq. (5.3).

where $\Lambda(\lambda)$ is a function of λ and the airfoil geometry. Thus, for a given material, geometry, and initial and final Mach numbers, the temperatures, stresses and effective torsional stiffness of the solid double-wedge airfoil are a function of the time parameter λ only. Non-dimensional temperatures, stresses, and Eq. (5.5) will be the same for model and prototype at corresponding values of λ. Since h appears in combination with the time t in the expression for λ, an incorrect Reynolds number, i.e., incorrect h, will merely affect the physical time at which the experimental results occur. Thus if the model Reynolds number is lower than the prototype value, similarity in T, σy, and GJ_{eff}/GJ_o will take place at a later time t for the model than for the prototype. The discussion so far has been restricted to an instantaneous acceleration from M_o to M_f. Ref. 24 also shows that for this airfoil the maximum loss in torsional stiffness, the most serious effect of the aerodynamic heating, is relatively unaffected by moderately rapid accelerations. The effect of Reynolds number relaxation then will be approximately the same for moderately rapid accelerations and for instantaneous accelerations.

Consider next the three cell built-up wing section of Fig. 7. Assume the skin temperature to be given by Eq. (5.2) and the web temperature at any instant to be given by

$$T_w(\xi) = T_{Aw}^{(0)} + \left[T_s - T_w(0) \right] \xi^n$$

$$(5.6)$$

where $\xi = \frac{z}{(d/2)}$. This assumes the temperature of the skin is unaffected by conduction to the web and is valid, as mentioned in Section 4.3, for skin-web joints of high thermal resistance. Applying the same assumptions as for the double-wedge profile, with h constant and for n positive, the stresses and the

effective torsional stiffness for this cross section are

$$\sigma_S = -E\alpha \Delta T_{AW} \left(1-e^{-\lambda}\right) \frac{A_w}{A_T} \left(\frac{m}{m+1}\right) \tag{5.7}$$

$$\sigma_W = E\alpha \Delta T_{AW} \left(1-e^{-\lambda}\right) \left[1 - \frac{A_w}{A_T}\left(\frac{m}{m+1}\right) - \xi^n\right] \tag{5.8}$$

$$\frac{GJ_{eff}}{GJ_o} = 1 + \frac{E\alpha \Delta T_{AW}}{G(\ell/d)^2} \Phi \tag{5.9}$$

where

$$\Phi = (1-e^{-\lambda})\left\{1 + \frac{A_w}{A_T}\left[4\left(\frac{\ell}{d}\right)^2 - 1\right]\right\}\left\{\left(\frac{\ell}{d}\right)^2\left(1-\frac{A_w}{A_T}\right) + \frac{A_w}{A_T} + \frac{1}{2}\left(\frac{m+1}{m+3}\right) - \frac{3}{2}\right\}$$

$$\frac{A_w}{A_T} = \frac{1}{1 + 2\frac{t}{d}\frac{\sigma_S}{\sigma_w}} \tag{5.10}$$

Again, as for the double-wedge, the Reynolds number appears through the time parameter λ in the temperatures, stresses, and GJ_{eff}/GJ_o expressions. The most serious situation for the built-up section regarding thermal stresses occurs when the webs are at their initial temperature while the skin is being rapidly heated. This corresponds to the case where $n \to \infty$. Φ then reduces to

$$\Phi = \frac{(1-e^{-\lambda})}{11}\left[\left(\frac{\ell}{d}\right)^2 - 1\right]\left\{1 + \frac{A_w}{A_T}\left[4\left(\frac{\ell}{d}\right)^2 - 1\right]\right\} \tag{5.11}$$

When $\ell/d \geq 1$, Φ in Eq. (5.11) is never negative, therefore this built-up section will experience no reduction in GJ_{eff}/GJ_o.

However, loss in torsional stiffness is quite likely if
the skin panels buckle locally under the action of thermal
stresses induced by large temperature differences between
the skins and webs.

The loss in torsional stiffness of a multiweb air-
foil with a double-wedge profile was studied in Ref. 25, in
which heat was conducted to the webs from the skin. The same
assumptions regarding flight history and skin temperature
were made as for the preceding two examples and again the
stresses and GJ_{eff}/GJ_0 were found to depend only on λ and geom-
etry. Fig. 8 shows $\Lambda(\lambda)$ calculated for this section for
various ratios of the web area to skin area and a heat trans-
fer-coefficient constant along the chord. The results show
that the loss in stiffness is less for the skin-web section
than for the solid double-wedge. In the limiting case where
there are no webs, $A_w/A_s = 0$, the section becomes a hollow
double-wedge and there is no loss in stiffness. This is a
consequence of the constant heat-transfer coefficient assump-
tion. Fig. 9 shows $\Lambda(\lambda)$ for a hollow section with a vari-
able h across the chord, for laminar and turbulent flow.
Though the reduction in stiffness is greater when h is vari-
able rather than constant across the chord, it is still sub-
stantially less than the reduction in stiffness for a solid
double-wedge.

In summary, for the specific cases considered here,
under the assumptions of rapid accelerations at constant
altitude, one-dimensional heat flow, elementary structural
theory, and constant material properties, the importance of
the Reynolds number with respect to temperatures, thermal
stresses, and loss in torsional stiffness resulting from
these stresses, is manifested in the time parameter $\lambda = \frac{z h_{\omega} t}{\rho_0 C_{p_0} l_0}$.
A distortion in the Reynolds number only affects the time t
at which the experimental results occur. Thermal similarity

thus is not affected.

The above results regarding the influence of
Reynolds number Re on specific models can be generalized to
other more arbitrary configurations. For general thin skin
built-up type wings, the assumption of the skin heating up
one-dimensionally with not much heat going into the webs
during early times (see discussion in Sections 4.2c) and
4.5), can be used to confine the incorrectly scaled Reynolds
numbers roughly to a redefinition of the reference time t_o
according to the parameter,

$$\frac{h\, t_o}{\rho_\theta\, C_{P_\theta}\, \delta_{os}} = \frac{.332 \sqrt{(R_e)}\, (P_r)^{1/3}\, k_o\, t_o}{\rho_\theta\, C_{P_\theta}\, \delta_{os}\, L} \quad \text{(laminar)} \tag{5.12a}$$

$$= \frac{.0296\, (R_e)^{4/5}\, (P_r)^{1/3}\, k_o\, t_o}{\rho_\theta\, C_{P_\theta}\, \delta_{os}\, L} \quad \text{(turbulent)} \tag{5.12b}$$

The aeroelastic properties of geometrically scaled, aerody-
namically heated models would then be similar at correspond-
ing times defined by Eq. (5.12), during the early period of
the heating up process. It is expected that the maximum
thermal stress effects will be encountered during this period.

The validity of all the previous similarity laws
and their relaxations should be checked by constructing sever-
al models, each at a different scale, and comparing their non-
dimensional responses under identical operating tunnel con-
ditions.

6. CONCLUSIONS

The present report has reviewed some of the basic similarity parameters for the general aerothermoelastic problem. The investigation was limited to moderate temperatures (below about $1000^\circ F$ - i.e., $M < 3.5$) and considered only elastic behavior of the material.

The similarity parameters for general aerothermoelastic phenomena in the above range were developed in Section 2, and are given by Eqs. (2.35). Certain inherent conflicts are present which permit similitude only for a scale ratio of 1. The primary conflict is between the M, Re, and P_0/E_0 conditions. For same materials and same temperatures, these three conditions can be satisfied only by a scale ratio of 1. Other less serious conflicts involving the characteristic time scale t_0, the radiation condition $\epsilon \cdot T_0^3 L / K_0$, and the Froude number U^2/gL are also present, but these are generally relatively minor.

To get around these conflicts, one may use different materials at different temperatures in different gases. This is discussed in Section 3. However, scale ratios L_p/L_m of only about 3 can be achieved in this manner by considering different materials, and scale ratios of about 5 by considering different gases.

Another means of getting around these is to develop less restrictive similarity parameters by considering more specialized situations. This is discussed in Section 4. When applied to a plate type structure, less restrictive parameters as given by Eq. (4.30) can be developed. Also, the consideration of heat conduction similarity in thin skin type structures at early times will lead to the parameters of Eq. (4.13). Conventional flutter, vibration, and buckling phenomena are also shown to be characterized by these specialized

similarity parameters. In Section 4.5, it is shown that geometrically distorted models can be constructed fulfilling these less restrictive similarity conditions.

A third approach to these conflicting similarity requirements is to leave one of the general parameters unsatisfied. This is discussed in Section 5. Consideration of the specialized situations above indicate that for geometrically scaled aeroelastic type models, it is most feasible to relax the Re requirement. For thin skin type models at early times, this incorrectly scaled Reynolds number results only in a redefinition of the time scale ratio according to Eq. (5.12).

For certain non-aeroelastic type tests in which the aerodynamic pressure distribution is known or can be estimated in advance, the P_o/E_o requirement can be replaced by the more general Eq. (2.40), and similarity can be achieved by placing additional external surface loads on the models. This is discussed at the end of Section 2.4.

The success with which each of the above approaches may be utilized to predict the performance of a prototype, depends on the specific situation involved and the understanding of what parameters may be of significance to the specific problem. In this connection, the use of "restricted" purpose models can be of considerable help in investigating clearly delineated problems. The validity of all the previous similarity laws and their relaxations should be checked by constructing several models, each at a different scale and comparing their non-dimensional responses under identical tunnel operating conditions.
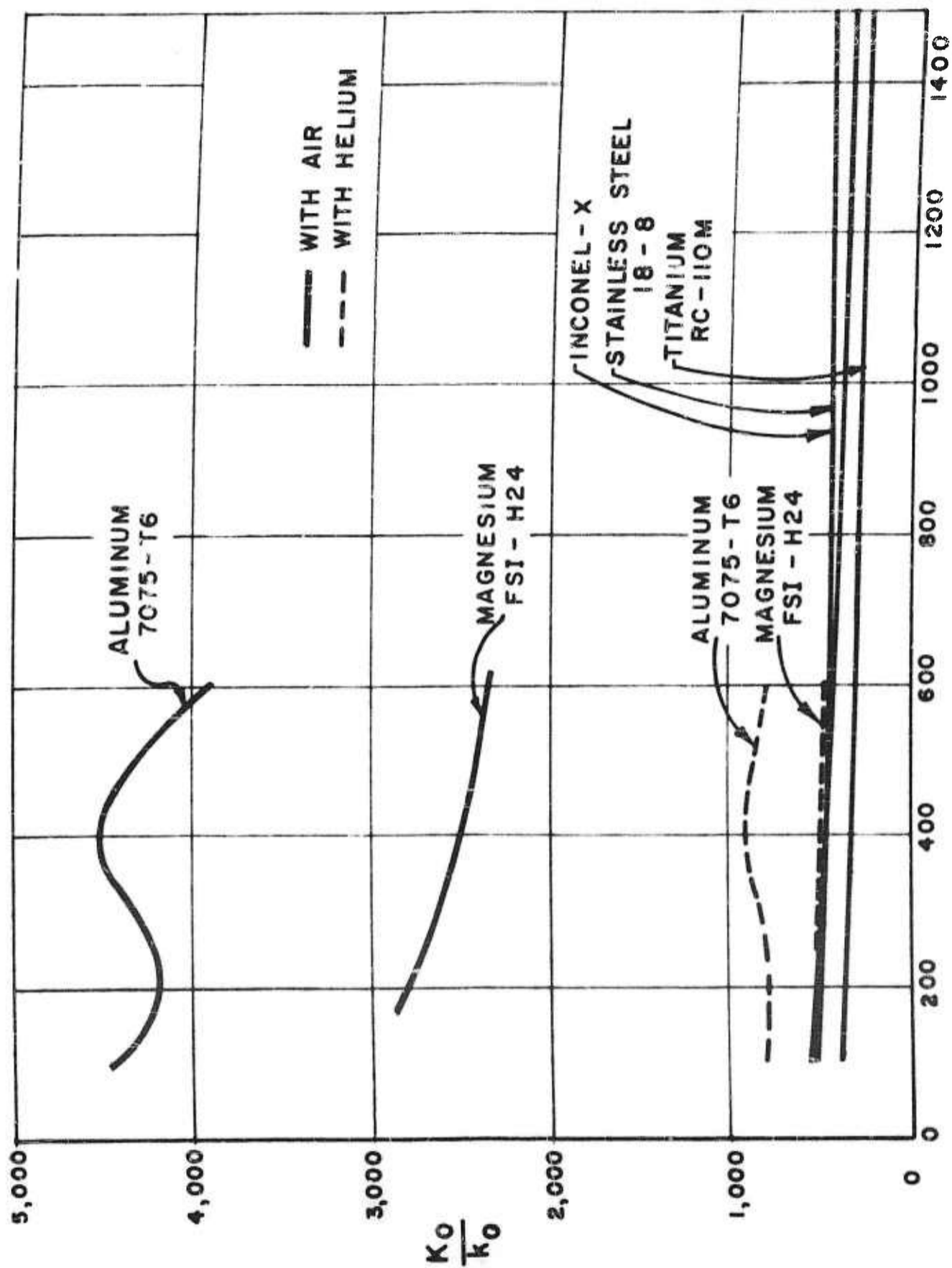
REFERENCES

1. Bisplinghoff, R. L., Some Structural and Aeroelastic Considerations of High Speed Flight, The Nineteenth Wright Brothers Lecture, Journal of the Aeronautical Sciences, Vol. 23, No. 4, April 1956.

2. Tsien, H. S., Similarity Laws for Stressing Heated Wings, Journal of the Aeronautical Sciences, Vol. 20, No. 1, January 1953.

3. Heldeniels, R. R., and Rosencrans, R., Preliminary Results of Supersonic - Jet Tests of Simplified Wing Structures, NACA RML53E 26a, July 8, 1953.

4. Mahoney, J. J., Some Aspects of Similarity Conditions for Supersonic Flows with Heat Transfer, S. M. Thesis, Department of Aeronautical Engineering, Massachusetts Institute of Technology, 1954.

5. Ting, L., Similarity Conditions for Testing High Speed Aircraft Models, Polytechnic Institute of Brooklyn, Department of Aeronautical Engineering and Applied Mechanics, PIBAL Report No. 308, AFOSR No. TN-56-548, November 1956.

6. O'Sullivan, W. J., Jr., Theory of Aircraft Structural Models Subject to Aerodynamic Heating and External Loads, NACA TN 4115, September 1957.

7. Scipio, L. A., II, and Teng, L. C., Analytical Study of Similarity Parameters for Aerodynamic Model Testing at High Temperatures, Part I - Similarity Criteria for Solid - and - Shell-Type Aerothermoelastic Models, WADC TR 57-496, ASTIA AD-142264, November 1957, Part II - Design Criteria for Wing-Type Aerothermoelastic Models, WADC TR 57-496, ASTIA AD 150 974, August 1957.

8. Molyneux, W. G., *Current Developments in Techniques for Wind Tunnel Aeroelastic Research*, RAE Internal Memorandum No. Structures 400, May 1958, (to be published).

9. Smith, J. A., Smiley, R. F., Vrablik, G. R., and Rossettos, J. N., *Studies Relating to the Field of Aero-thermoelasticity, Part II, A survey of Aerothermoelastic Phenomena*, WADC TR 57-529, ASTIA AD 155812, August 1958, (CONFIDENTIAL).

10. Hoff, N. J., Editor, *High Temperature Effects in Aircraft Structures, Chapter 16, Models and Analogs*, (by R.R. Heldenfels) NATO, AGARD, AGARDograph No. 28, New York, Permagon Press, 1958.

11. Bogdonoff, S. M., and Hammitt, A. G., *The Princeton Helium Hypersonic Tunnel and Preliminary Results Above M = 11*, WADC TR 54-124, ASTIA AD 55668, July 1954.

12. Chapman, D. R., *Some Possibilities of Using Gas Mixtures Other Than Air in Aerodynamic Research*, NACA TR 1259, 1956.

13. Keyes, F. G., *The Heat Conductivity, Viscosity, Specific Heat and Prandtl Number for Thirteen Gases*, Massachusetts Institute of Technology, Project Squid, Report 37, April 1952.

14. von Doenhoff, A. E., Braslow, A. L., and Schwartzberg, M.A., *Studies of the Use of Freon - 12 as a Wind-Tunnel Testing Medium*, NACA TN 3000, August 1953.

15. Ashley, H., and Zartarian, G., *Piston Theory - A New Aerodynamic Tool for the Aeroelastician*, Journal of the Aeronautical Sciences, Vol. 23, No. 12, December 1956.

16. Liepmann, H. W., and Roshko, A., *Elements of Gas-dynamics*, John Wiley and Sons, Inc., New York 1957.

17. Hayes, W. D., and Probstein, R. F., _Viscous Hypersonic Similitude_, IAS Preprint No. 59-63, Presented at the Institute of Aeronautical Sciences Annual Meeting, New York, New York, January 26-29, 1959.

18. Lees, L., _Hypersonic Flow_, JAS-RAeS Fifth International Aeronautical Conference, Los Angeles, Preprint 554, June 20-24, 1955.

19. Lighthill, M. J., _Contributions to the Theory of Heat Transfer Through a Laminar Boundary Layer_, Proceedings of the Royal Society A, Vol. 202, No. 1070, August 1950.

20. Eckert, E. R. G., Hartnett, J. P., and Birkebak, R., _Simplified Equations for Calculating Local and Total Heat Flux to Nonisothermal Surfaces_, Journal of the Aeronautical Sciences, Vol. 24, No. 7, July 1957.

21. van Driest, E. R., _The Problem of Aerodynamic Heating_, Aeronautical Engineering Review, October 1956.

22. Bisplinghoff, R. L., Ashley, H., and Halfman, R. L., _Aeroelasticity_, Addison - Wesley Publishing Company, Inc., Cambridge, Massachusetts, 1955.

23. Hedgepeth, J. M., _Flutter of Rectangular Simply Supported Panels at High Supersonic Speeds_, Journal of the Aeronautical Sciences, Vol. 24, No. 8, August 1957.

24. Budiarsky, B., and Mayers, J., _Influence of Aerodynamic Heating on the Effective Torsional Stiffness of Thin Wings_, Journal of the Aeronautical Sciences, Vol. 23, No. 12, December 1956.

25. Thomson, R. G., _Effects of Cross-Sectional Shape, Solidity, and Distribution of Heat-Transfer Coefficient on the Torsional Stiffness of Thin Wing Subjected to Aerodynamic Heating_, NASA MEMO. 1-30-59L, February 1959.

26. Dukes, W. H., and Schnitt, A., Editors, <u>Structural Design for Aerodynamic Heating, Part I, Design Information</u>, WADC TR 55-305, Part I, October 1955, (CONFIDENTIAL).

27. Bryant, J. M., Roach, R. E., and Donaldson, J. E., <u>Physical Properties of Aircraft Structural Materials at Elevated Temperatures</u>, Chance Vought Aircraft Rpt. 9112, Vols. I and II, June 1955.

28. Johnston, G. S., <u>A Study of Materials Operating at Elevated Temperatures</u>, Bell Aircraft Corporation, Report 02-941-024, Revised, April 1952.

FIG.1 THE PARAMETER $\frac{K_0}{k_0}$ AS A FUNCTION OF THE REFERENCE TEMPERATURE T_0

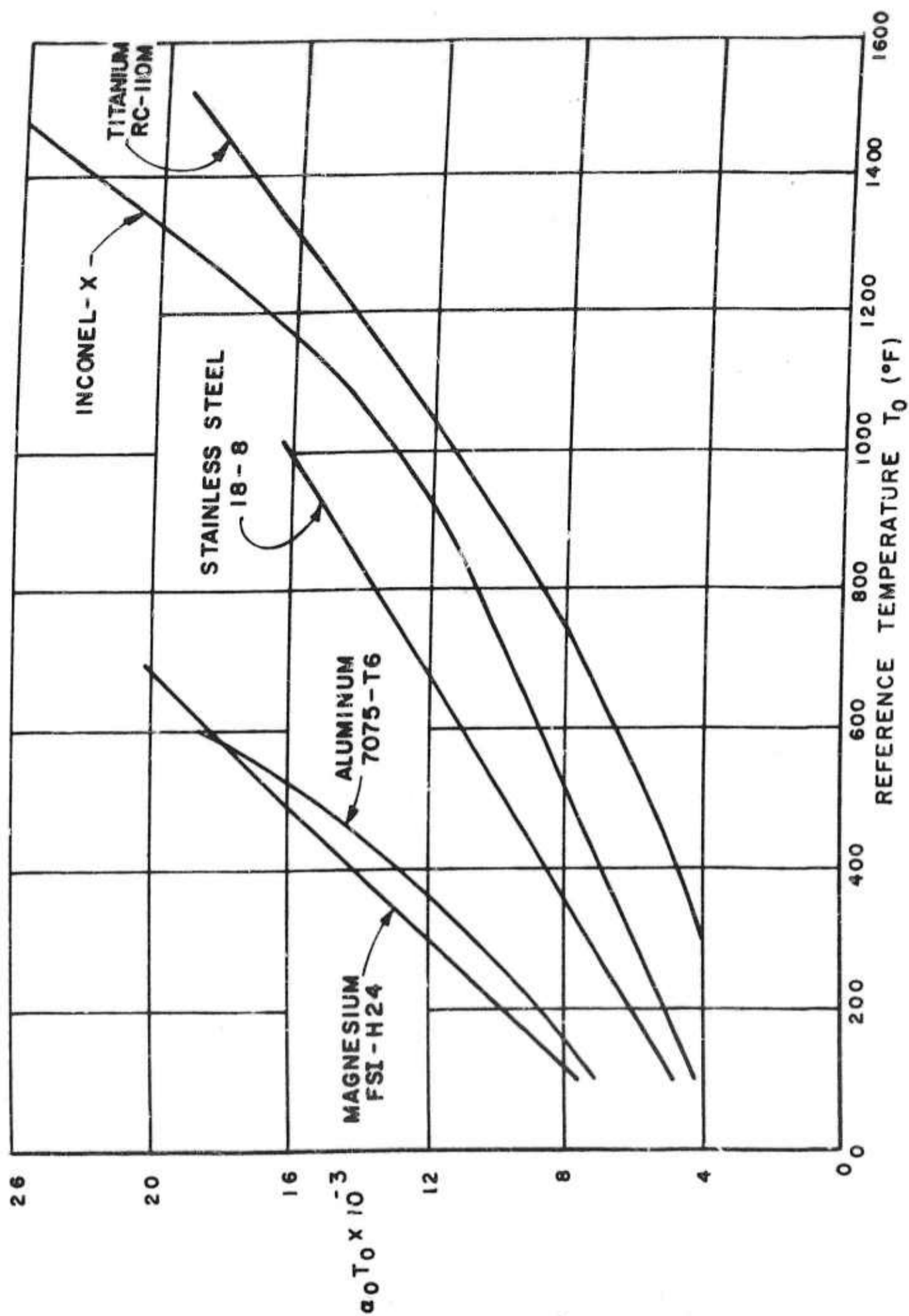FOR FIVE STRUCTURAL MATERIALS

FIG. 2 THE PARAMETER $\alpha_0 T_0$ AS A FUNCTION OF THE REFERENCE TEMPERATURE T_0 FOR FIVE STRUCTURAL MATERIALS
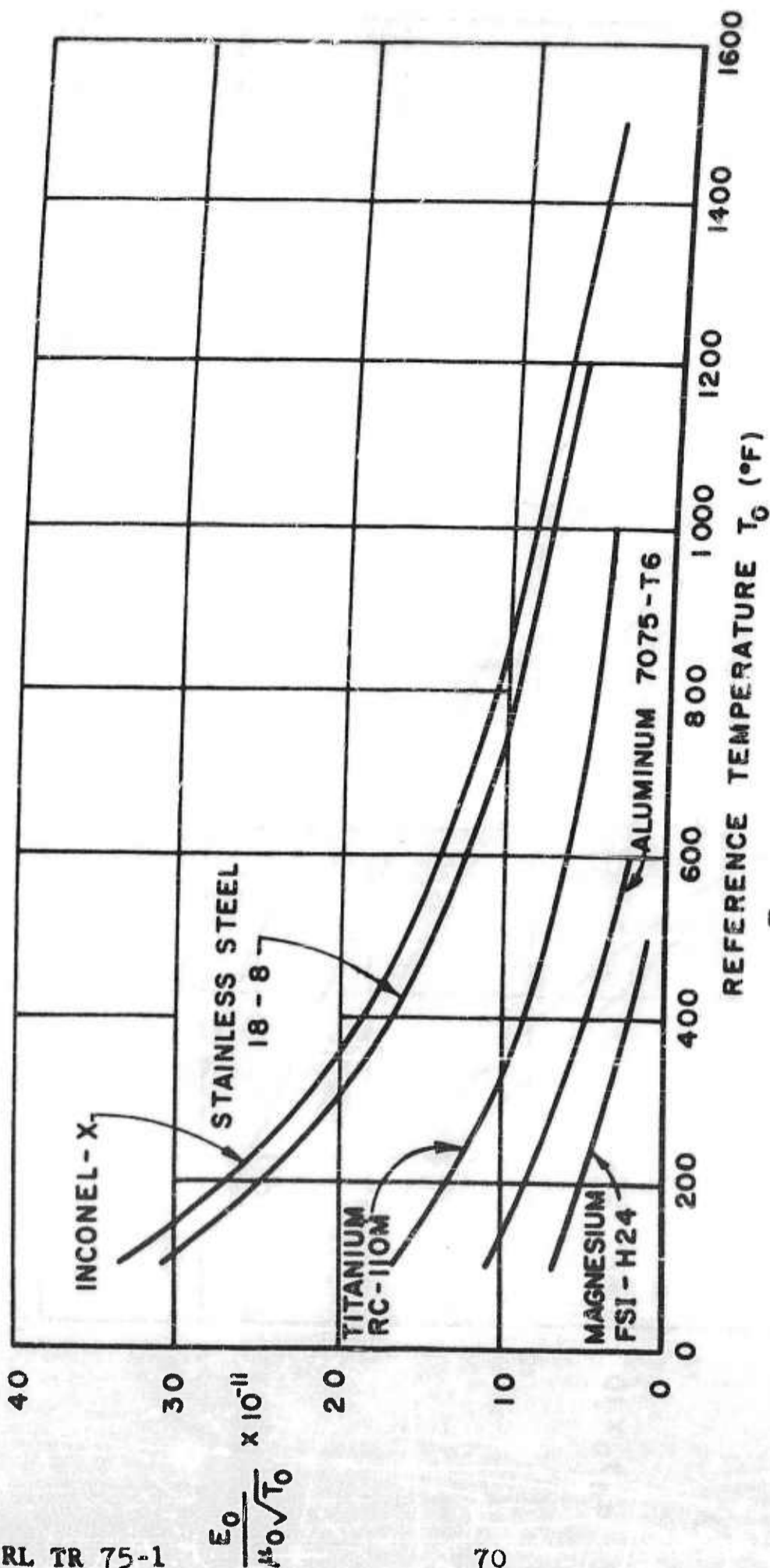
FIG. 3 THE PARAMETER $\dfrac{E_0}{\mu_0 \sqrt{T_0}}$ AS A FUNCTION OF THE REFERENCE

TEMPERATURE T_0 FOR FIVE STRUCTURAL MATERIALS AND AIR AS THE

GAS MEDIUM

Aluminum Prototype, $(T_o)_P = 400°F$

Model	$(T_o)_M$, °F	$\dfrac{(K_o/k_o)_m}{(K_o/k_o)_p}$	$\dfrac{(\alpha_o T_o)_m}{(\alpha_o T_o)_p}$	L_P/L_M
Aluminum	100	1.0	.55	2.2
Magnesium	100	.65	.63	1.4
Inconel-x	100	.11	.33	6.7
Inconel-x	980	.10	1.0	1.8

Inconel-x Prototype, $(T_o)_P = 1000°F$

Model	$(T_o)_M$, °F	$\dfrac{(K_o/k_o)_m}{(K_o/k_o)_p}$	$\dfrac{(\alpha_o T_o)_m}{(\alpha_o T_o)_p}$	L_P/L_M
18-8 Steel	750	.87	1.0	1.15
Titanium	300	.73	.31	2.30
Aluminum	100	9.7	.54	1.25

Titanium Prototype, $(T_o)_P = 800°F$

Model	$(T_o)_M$, °F	$\dfrac{(K_o/k_o)_m}{(K_o/k_o)_p}$	$\dfrac{(\alpha_o T_o)_m}{(\alpha_o T_o)_p}$	L_P/L_M
18-8 Steel	400	1.6	1.0	3.4
Inconel-x	600	1.5	1.0	2.1
Titanium	100	1.3	.35	3.4

18-8 Stainless Steel Prototype, $(T_o)_P = 800°F$

Model	$(T_o)_M$, °F	$\dfrac{(K_o/k_o)_m}{(K_o/k_o)_p}$	$\dfrac{(\alpha_o T_o)_m}{(\alpha_o T_o)_p}$	L_P/L_M
Inconel-x	100	1.0	.31	3.5

Figure 4 Satisfying the General Similarity Parameters M, R_e, P_o/E_o, K_o/k_o, $\alpha_o T_o$

Gas	γ	m, gms/mole	μ, poises $\times10^5$ at 0°C,	$\frac{\mu_{air}}{\mu_{gas}}\sqrt{\frac{(\gamma m)_{gas}}{(\gamma m)_{air}}}$	P_r at 0°C	$\frac{k}{(k)_{air}}$ 0°C
Air	1.40	29	17.2	1.00	.72	1.0
Helium	1.67	4	18.6	.38	.68	5.9
Argon	1.67	40	21.0	·1.05	.66	.68
Carbon Dioxide	1.30	42	13.7	1.46	.78	.60
Krypton	1.68	84	23.0	1.40	-	-
Xenon	1.67	131	21.0	1.91	-	-
Freon 12	1.13	121	11.8	2.68	.83	.34
Freon 13B1	1.15	149	14.3	2.48	-	-
C_4F_{10}	1.06	238	11.1	3.86	-	-
CB_rF_3 and Argon	1.40	76	17.7	1.56	-	-
SF_6 and Argon	1.40	72	17.9	1.52	-	-
CF_4 and Argon	1.40	68	18.4	1.43	-	-

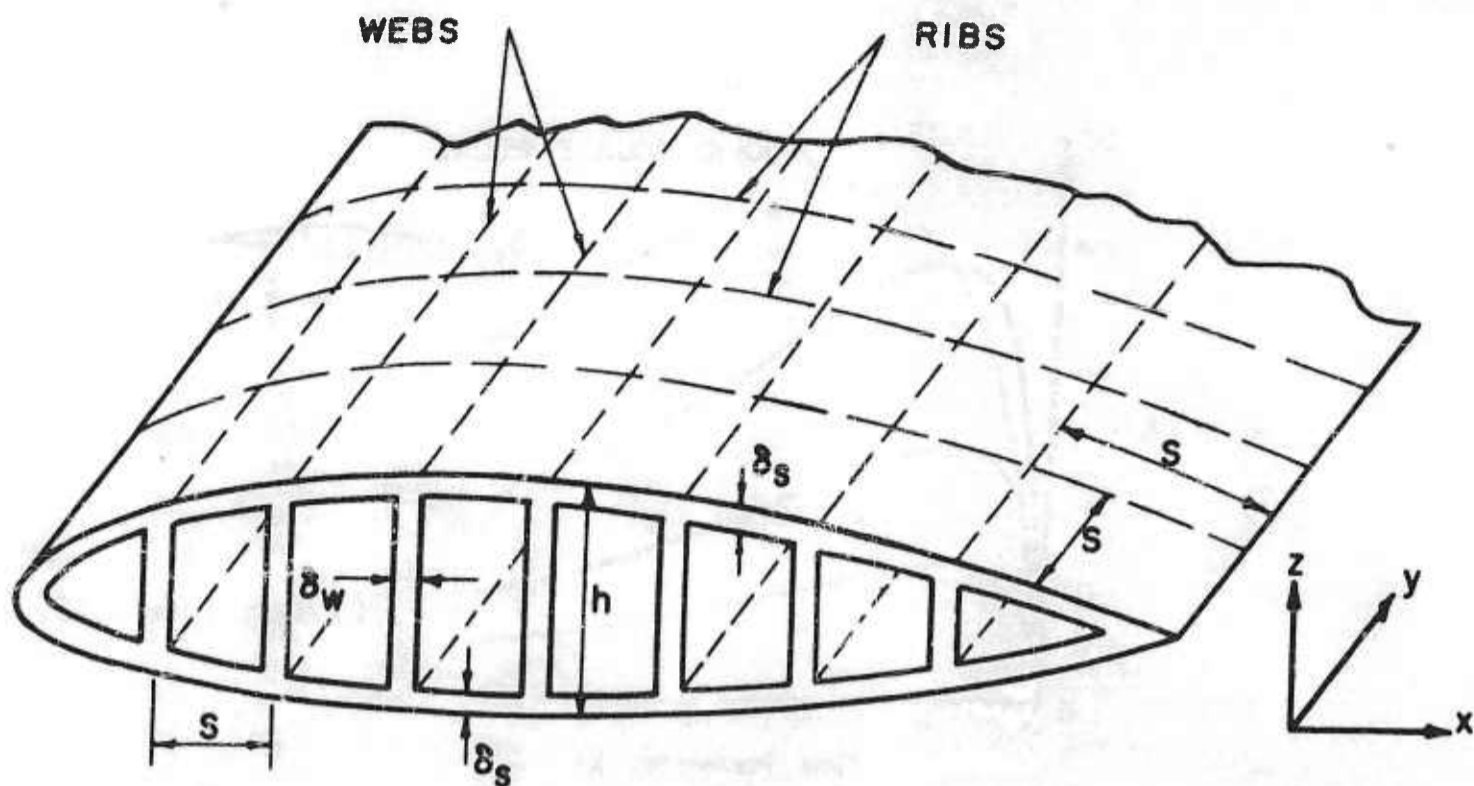Figure 5 Properties of Some Possible Substitute Gases

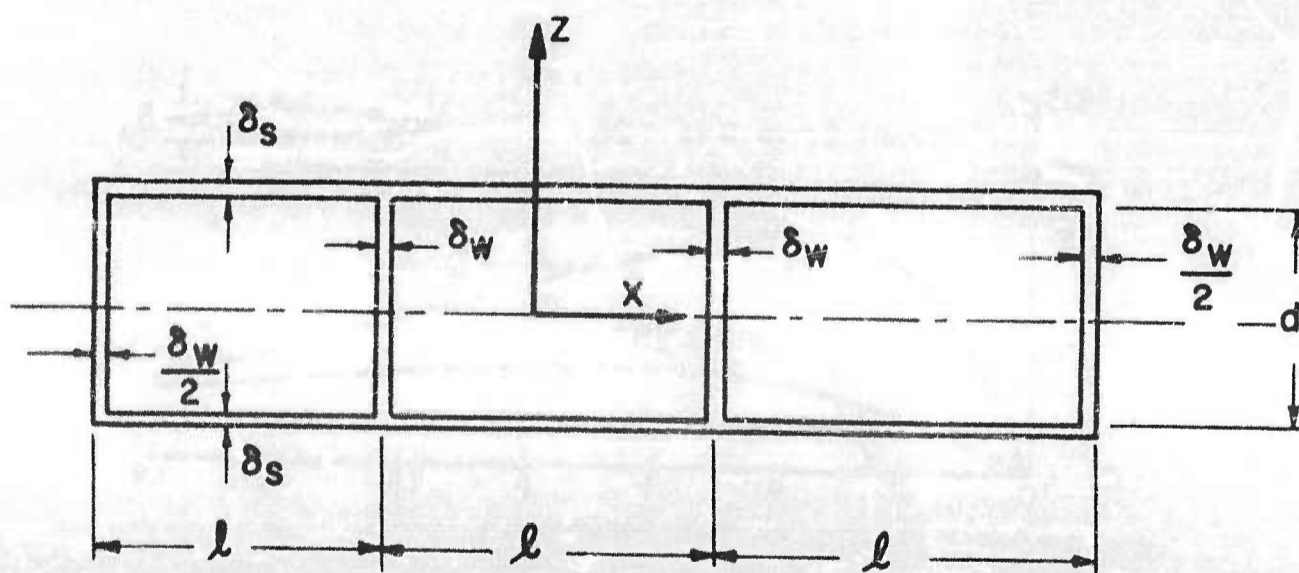FIG. 6   LOW ASPECT   RATIO   BUILT-UP   WING

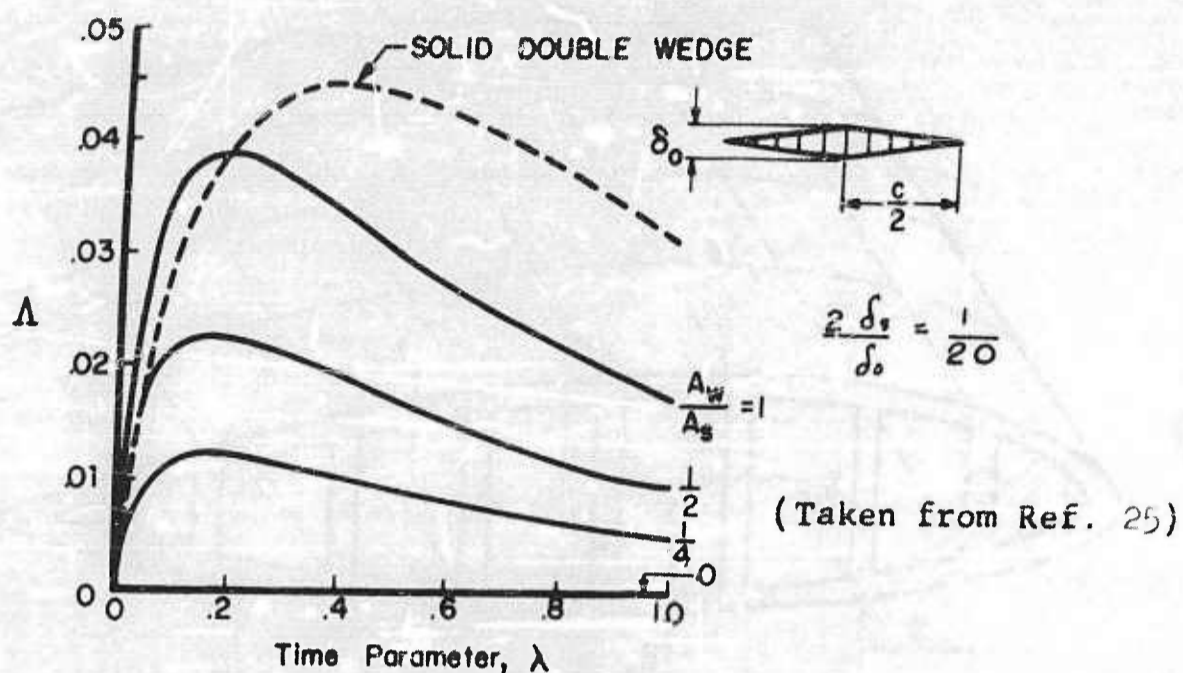FIG. 7   THREE CELL   BUILT-UP   WING SECTION

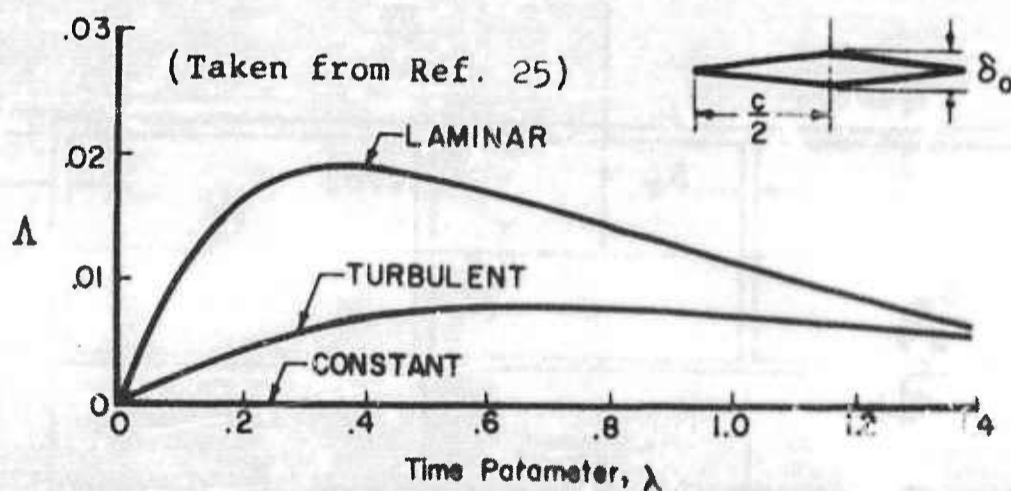FIG. 8 TORSIONAL STIFFNESS REDUCTION OF A MULTIWEB AIRFOIL.

FIG. 9 EFFECT OF A VARIABLE HEAT TRANSFER COEFFICIENT ON TORSIONAL STIFFNESS OF A HOLLOW DOUBLE-WEDGE AIRFOIL.